

Towards the ambient aerosol extinction from dried aerosol in situ observations

by

P. M. van Binsbergen

to obtain the degree of Master of Science
at the Delft University of Technology,
to be defended publicly on Monday December 16, 2019 at 13:30.

Student number: 4227743
Project duration: April 17, 2019 – December 6, 2019
Thesis committee: Dr. G. (George) Biskos TU Delft, supervisor
Dr. J.S. (Bas) Henzing TNO
Prof. dr. ir. H. (Herman) Russchenberg TU Delft
Dr. S.R. (Stephan) de Roode TU Delft

An electronic version of this thesis is available at <https://repository.tudelft.nl/>.



Abstract

Accurate predictions of the extinction and scattering properties of the atmosphere are important for climate research and interpreting satellite data. This study introduces a model (called the H-model) that calculates the scattering coefficients and scattering enhancement factors based on in situ measurements of the dried ambient aerosol. A disadvantage of using dried aerosol measurements is that they do not correspond with the ambient conditions, as they are measured at a relative humidity below 40% and thus the particles are assumed to contain no water. Measurements of aerosol chemical composition do not contain water mass concentrations and measurements of the particle size distribution do not include water. To solve this problem, the H-model uses ISORROPIA, a thermodynamic equilibrium model, to estimate the expected amount of aerosol water content and growth factor $g(\text{RH})$ of aerosol particles for any given temperature and relative humidity (RH). With this information, the conversion between dry and enhanced relative humidity can be made. The chemical composition measurements can be complemented with the estimated aerosol water concentrations and the particle size distribution can be recalculated based on the growth factor for any given RH. In addition, the growth factor is also calculated by using k-Köhler theory and compared to the results of ISORROPIA. The findings of this sub-study show that the growth factors calculated by both approaches (ISORROPIA and k-Köhler theory) are similar as they significantly correlate. ISORROPIA, however, is more sensitive to small chemical changes which makes it more appropriate for the H-model.

The calculated growth factors are used in the H-model to estimate changes in the chemical composition and particle size distribution of the aerosol particles at enhanced relative humidity. Subsequently, the H-model uses MIE theory to estimate the scattering properties of the particles at a specific relative humidity. By doing so, the scattering properties can be calculated at dry and enhanced RH, making it possible to calculate scattering enhancement factors. Finally, the H-model is validated by comparing the calculated scattering properties to measured scattering properties of a (humidified) nephelometer. To do so, in situ measurements from the CINDI campaign in 2009 and the TROLIX campaign in 2019 at Cabauw are used. The findings of this validation show that the results from the H-model do not yet accurately match the measurements. That being said, a strong correlation is observed between the calculated and the measured scattering properties. This shows that the H-model is able to capture changes in the particle size distribution and chemical composition while calculating the enhancement factors. It can be concluded that the results from the H-model are promising but need further work to close the gap between the calculations and measurements. The H-model makes multiple simplifications and assumptions which could be improved upon, thereby increasing the precision of the results as well. Furthermore, to fully conclude the findings of this study, the measurements of the SMPS and the nephelometers should be calibrated. A better statement can then be made about the accuracy of the comparison between the scattering properties calculated by the H-model and measured by the nephelometers.

Contents

1	Introduction	1
2	Background and Theory	3
2.1	Aerosol optical properties	3
2.2	Aerosol hygroscopicity	4
3	Model framework development	6
3.1	Model	6
3.1.1	Model steps	6
3.2	Sub-models used in the H-model	8
3.2.1	ISORROPIA [D]	8
3.2.2	Mie model [I]	8
3.3	Input/Output variables	10
3.3.1	Chemical composition (dry) [A]	10
3.3.2	Temperature and Relative Humidity [B]	11
3.3.3	Particle Size distribution (dry) [C]	11
3.3.4	Refractive index [G]	12
3.3.5	Particle size distribution (wet) [H]	13
3.3.6	Enhancement factors [J]	13
4	Model validation	14
4.1	Model test run and comparison with measurements from the CINDI campaign	14
4.1.1	Input data	14
4.1.2	Results from the CINDI campaign	16
4.2	Sensitivity analysis	19
4.2.1	ISORROPIA-aerosol species combinations	19
4.2.2	Sensitivity of the ISORROPIA model	21
4.3	Model run and comparison with measurements from the TROLIX campaign	22
4.3.1	Input data	22
4.3.2	Data processing	24
4.3.3	Results from the TROLIX campaign	28
5	Discussion and conclusion	39
5.1	Discussion	39
5.1.1	Discussion on the H-model	39
5.1.2	Discussion on the input values	40
5.1.3	Discussion on the nephelometers	41
5.2	Conclusions	42
A	List of acronyms and abbreviations	43
	List of Figures	44
	List of Tables	45
	Bibliography	46

1 Introduction

Aerosol particles are an important element in light absorption and scattering of the atmosphere. As light propagates through the atmosphere it interacts with everything it encounters, including aerosol particles. Part of the light is scattered or absorbed by the particles in the air. Light scattering by gases, as opposed to aerosol particles, can be easily estimated as it is a well-known process, the intensity of which is proportional to the air density. Light scattering and absorption by aerosols is more complicated as it depends on the amount of particles, their specific size, shape and chemical composition. Because of their scattering and absorbing properties, aerosol particles have a direct impact on the radiative properties of the atmosphere and with that an effect on climate change. Of all the components contributing to radiative forcing, aerosol particles are associated with the highest uncertainty and are therefore important to fully understand (Myhre et al., 2013). Knowledge of aerosol optical and radiative properties is essential for understanding this problem and the effects of aerosols on the climate.

Aerosol particles in the atmosphere can be described in different ways. The particle size distribution gives the amount of particles present in the air within a specific size range. The chemical composition gives the mass amount of different species present in the air. The particle size distribution and chemical composition are interdependent, but can be affected by relative humidity and temperature. The amount of scattering and absorption by the aerosol particles is thus a function of particle size distribution, chemical composition, relative humidity and temperature. Measuring and analysing these aerosol properties can help us to assess the effects of aerosol particles on light scattering and the climate forcing. Ideally, aerosol properties are measured at ambient conditions so they are representative of the 'real' situation. However, aerosol in situ measurements are often measured in dry state which means that the ambient air is dried to a relative humidity (RH) below 40%, so that the aerosols contain a low amount of water and thus the hygroscopic growth of the particles is minimized (Kazadzis, 2016). As a result, measuring aerosol properties at $RH < 40\%$ makes it easier to compare measurements between different locations, considering that higher RH values can create large differences in e.g. optical properties. However, as a consequence of dry measurements, the results are not representative for the ambient conditions which are measured by e.g. remote sensing (satellites). To close the gap between measurements of aerosol particles at dried and ambient conditions, a correction needs to be made between dry and elevated RH values. To perform this correction, enhancement factors are used. The scattering enhancement factors $f(RH)$ describe the enhancement of the scattering properties due to an enhanced relative humidity.

In order to determine the enhancement factor, an integrated model is needed that captures the scattering properties of aerosol particles. Most importantly, it needs to capture the change in scattering properties based on the hygroscopic growth at specific RH conditions. The model developed in this report is based on known aerosol and scattering theory, such as the MIE theory, and includes existing models such as ISORROPIA to estimate water uptake by aerosols. Based on dry in situ measurements of the chemical composition and particle size distribution, the model calculates the scattering coefficients. To calculate those scattering coefficients at enhanced relative humidity, an estimation of the amount of aerosol water content is needed at that specific relative humidity. The amount of water on the particles influences their chemical composition and size. The aerosol water content can be estimated based on the dry chemical composition and RH. With increasing RH, the aerosols will grow when they take up water, causing changes in the particle size distribution. Based on the (dry) measured particle size distribution and the growth factor as calculated by the water content increase, a new (wet) particle size distribution can be established. Changes in the water content of the aerosol particles will change the value of the refractive index of the aerosol as well. The altered size distribution and refractive index are used to estimate extinction and scattering values for any value of relative humidity between 0 and 100%. A scattering enhancement factor can then be calculated as the scattering coefficients can be calculated for aerosol compositions at specific RH conditions. The enhancement factor describes then the direct relationship between dry (in situ) measurements and enhanced ambient conditions. The enhancement factor can be estimated by a humidified nephelometer as well (Zieger et al., 2011). In this study the results from the humidified nephelometer and the model based on dry in situ measurements (the H-model) will be compared to validate the model: to see if the model calculates realistic values.

The goal of this study is to build a model that can calculate scattering properties at any given relative humidity, in order to estimate scattering enhancement factors. The model calculates these values using as an input the dry in situ measurements of size distributions and chemical composition. The study is divided over two main parts. The first part covers the design of the model, describing which input variables are needed and which models or theories are used within the model. The second part investigates the capability of the model and checks whether it is able to correctly estimate the scattering properties. To answer this question, predictions from the model are compared with measurements from the CINDI and TROLIX campaign where data from nephelometers operated at dry and humidified conditions were carried out.

The following structure is used: Chapter 2 provides background information on aerosol optical properties and aerosol hygroscopicity. Both are important terms to understand how extinction and scattering in ambient conditions are estimated. The model that is used to estimate the scattering properties is explained in chapter 3. Chapter 4 contains the validation of the model, it contains the results of the first model test run based on CINDI campaign data (2009), a sensitivity study and a final model run with data based on measurements made during the TROLIX campaign (from 10/09/2019 until 07/10/2019). The main conclusions from the results are provided in chapter 5.

2 Background and Theory

2.1 Aerosol optical properties

Aerosols are a suspensions of liquid and solid particles in the atmosphere with particle sizes ranging from approximately $10^{-3} \mu\text{m}$ to $10 \mu\text{m}$ in diameter. When a ray of light propagates through the atmosphere, its pathway can intersect with that of an aerosol particle, resulting in two possible processes:

- The light is absorbed by the aerosol
- The light is scattered away from the aerosol

Both light absorption and scattering contribute to the overall extinction of light through the aerosol. The amount of light that gets extinct due to the aerosols in the air can be expressed by the light extinction coefficient σ_e [m^{-1}] which depends on the scattering coefficient σ_s [m^{-1}] and absorption coefficient σ_a [m^{-1}].

$$\sigma_e = \sigma_s + \sigma_a \quad (2.1)$$

Each of these coefficients describes the effective total aerosol cross section within a given air volume. The extinction optical depth can be calculated by multiplying the corresponding coefficient with the total path length of a light bundle through the medium with the extinction coefficient. The same goes for the scattering or absorption coefficient.

Scattering and extinction coefficients are largely dependent on the particle size distribution, the aerosol chemical composition and the wavelength(s) of the incoming light. The aerosol scattering coefficient (σ_s) is a function of particle cross section (G) and the corresponding scattering efficiency (Q_s).

$$\sigma_s = Q_s \cdot G \quad (2.2)$$

Similarly, the aerosol extinction coefficient (σ_e) is a function of the particle cross section G and the corresponding extinction efficiency (Q_e)

$$\sigma_e = Q_e \cdot G \quad (2.3)$$

where G is the total particle cross section of the particles:

$$G = \sum_{i=1}^n \pi r_i^2 \quad (2.4)$$

Here n is the total number of aerosol particles and r_i the radius of the particle. As a result, the total particle cross section depends on the particle size distribution. Once aerosols start to take up water, the particles grow in size and so the particle cross section increases.

Determining the extinction or scattering efficiency (Q_e , Q_s) is more complex compared to the particle cross section, as it depends on the particle size distribution, the aerosol chemical composition and the wavelength(s) of the incoming light. How light scatters off particles depends on the wavelength and particle size, captured together in the size-parameter. Interaction of light with the particles can be described by Rayleigh, Mie or geometrical optics, depending on the relative size of the particle (radius-to-wavelength-ratio). The so-called size-parameter $\frac{2\pi r}{\lambda}$ (with r the radius of the particle and λ the wavelength of the incoming radiation) defines the different regions. For particles much smaller than the wavelength ($2\pi r \ll \lambda$), the process can be described by Rayleigh scattering. An example of this is how sunlight scatters off molecules in the atmosphere, causing a blue sky in the process. For particles significantly larger than the wavelength ($2\pi r \gg \lambda$), such as raindrops, geometrical optics can be used. For particles with roughly the same size as the used wavelength ($2\pi r \approx \lambda$) the process is called Mie scattering. This is also where the majority of aerosol scattering takes place, as aerosol diameters are of the same order of magnitude as the wavelengths of the incident sunlight. The Mie region describes the region where the scattering efficiency is oscillatory with the size parameter. The interaction of (sun)light with aerosols is described by the Mie theory (Mie

solution of Maxwell's equations). Assuming a homogeneous spherical particle, Mie theory calculates the scattering and extinction efficiency for a specific aerosol particle. The outcome mainly depends on the radius-to-wavelength-ratio, see Figure 2.1. Figure 2.2 shows the radius dependency of the efficiency for $\lambda = 550\text{nm}$. Calculating scattering values becomes very complex in this regime as there is no simplified relation for a particle or an entire particle size distribution. A slight change of the particle size distribution can result in a large difference in the scattering efficiency of the particles due to this oscillatory behaviour in the Mie region. With enough data on the particle size distribution and chemical composition it is possible to calculate these changes with the MIE-model.

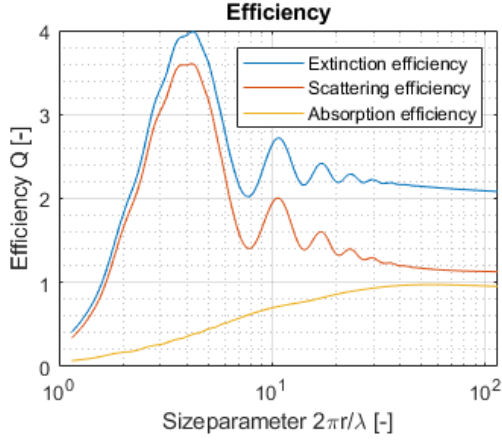


Figure 2.1: Example of the efficiency Q ($\sigma/\pi r^2$) as a function of the size parameter ($\frac{2\pi r}{\lambda}$) for $RI=1.5$ $0.02i$.

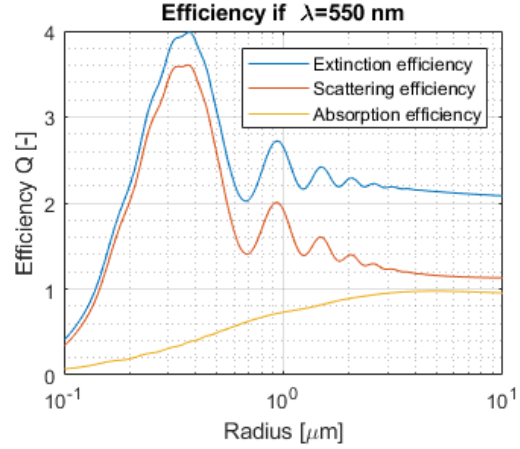


Figure 2.2: Example of efficiency Q ($\sigma/\pi r^2$) as a function of the aerosol particle radius [μm] for $RI=1.5$ $0.02i$.

Aerosol optical properties are significantly influenced by relative humidity. To quantify this influence, we can use an enhancement factor. The scattering enhancement factor $f(RH)$ is defined as:

$$f(RH, \lambda) = \frac{\sigma_s(RH, \lambda)}{\sigma_s(RH_{dry}, \lambda)} \quad (2.5)$$

In this equation σ_s is the scattering coefficient at a given RH and with a given wavelength λ . The enhancement factor describes the dependence of scattering or extinction coefficient (σ_s, σ_e) on relative humidity. It is expressed as a multiple of the value under the dry conditions. This study mainly focuses on the scattering enhancement $f(RH)$. Substituting Equation 2.2 in Equation 2.5 (while assuming a fixed wavelength) yields:

$$f(RH) = \frac{G(RH)}{G(RH(dry))} \cdot \frac{Q(RH)}{Q(dry)} = G_{enhancement} \cdot Q_{enhancement} \quad (2.6)$$

This shows that the scattering enhancement depends on the enhancement in total aerosol cross section ($G_{enhancement}$) and the change of efficiency ($Q_{enhancement}$). The efficiency enhancement can also be smaller than one, this depends on the size and the growth of the aerosol particle or particle size distribution (PSD).

2.2 Aerosol hygroscopicity

Most aerosol species absorb water from the air if the relative humidity (RH) is large enough. With increasing water vapour, hygroscopic aerosols take up water and grow in size. Sea salts and some inorganic aerosols are highly hygroscopic aerosols (Topping et al., 2004). Other species such as carbon or mineral dust do not take up any water at sub-saturated ($RH < 100\%$) conditions. As a result, the hygroscopicity of an aerosol mixture can vary widely depending on the chemical composition.

In general, a hygroscopic particle will take up more water with increasing RH and lose liquid water with decreasing RH. This transition differs for all aerosol species. Some particles will start to take up water with only low amount of water vapour available (at low RH), other particles need a larger RH to trigger the water uptake. Some aerosols such as sea salt particles are known for having a deliquescent and efflorescent behaviour. This behaviour can be recognized by a sudden growth or decrease of the size of a particle at a given RH. The deliquescence point describes the RH at which the particle will suddenly change from their crystalline form to their liquid form if the RH is increased. The efflorescence point describes the RH at which the particle will change from its liquid form to its crystalline form. The efflorescence point can have a much lower value than the deliquescence point. For a given RH it is thus possible to have crystallized or dissolved salt particles, which depends on the original state (crystallized or liquid) of the particles. This is relevant because the size of the particles and the amount of aerosol water depend on the state of the aerosol and the RH history. An example can be seen in Figure 2.3 (Gupta et al., 2015) where the growth of a NaCl particle is visualized for humidification and dehydration of this specific particle.

Ambient aerosol compositions in the Netherlands often contain a certain amount of sea salts. Especially with western wind, a relatively large part of the aerosol composition consists of sea salt particles. The deliquescent behaviour of the aerosol can affect the mean growth-factor of the entire aerosol composition as shown in Figure 2.4 (Boreddy et al., 2014). It is important to know whether the particles contain species that can deliquesce and if so, whether the measured particles are from the dehydration or hydration branch (so if the original state of the particle is crystallized or liquid). Under normal conditions it can be assumed that most deliquescent aerosols are in the dehydration branch because ambient air conditions have a high enough relative humidity to not go below the efflorescence point.

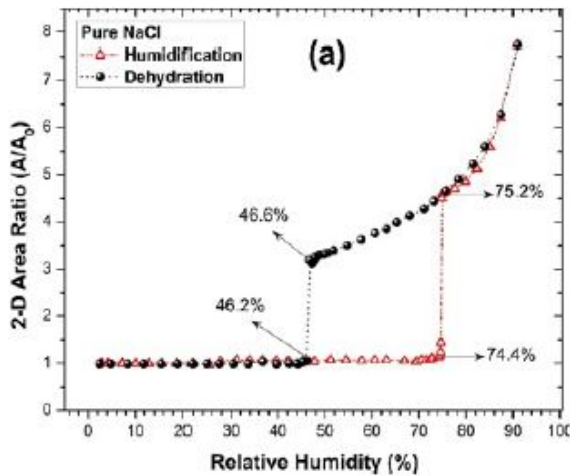


Figure 2.3: Example of the deliquescent behaviour of a NaCl particle: 2D area growth of NaCl as a function of RH. (Gupta et al., 2015)

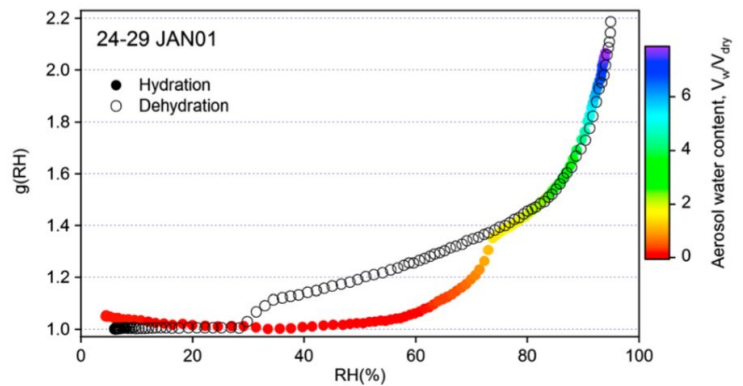


Figure 2.4: Example of an aerosol mixture whose growth factor is influenced by the presence of aerosols with a deliquescent behaviour: Diameter growth factor (G) as a function of RH. (Boreddy et al., 2014)

3 Model framework development

3.1 Model

During this study a model is created to calculate scattering, extinction and enhancement values from dried aerosol in situ measurements. The most important part of the model is the calculation of the water (H₂O) uptake of the aerosols and its effect on the PSD and chemical composition which determine the enhancement factor. Therefore this model will be referred to as the H-model, short for H₂O-model. Existing theories and models are combined to create the H-model which will be further explained in section 3.2.

3.1.1 Model steps

The H-model calculates the scattering coefficients of aerosol particles under different conditions. The different steps and components of the model are shown in Figure 3.1 and will be briefly described below. A more detailed explanation of the input and output variables of the individual components can be found in section 3.2 and section 3.3.

Input

Blocks [A], [B] and [C] describe the input variables, these are the (dry) chemical composition of the aerosol particles (CC), the dry particle size distribution (PSD), the temperature (T) and Relative Humidity (RH). The H-model calculates the scattering coefficients based on these variables. By changing, for example, the RH and keeping the other variables constant, the scattering coefficient at different RH values can be calculated and therefore the enhancement factor.

From dry to elevated relative humidity conditions

Using the model ISORROPIA [D] (Fountoukis and Nenes, 2007), the amount of liquid aerosol water [E] can be estimated depending on the chemical composition, RH and temperature. An increase in water volume changes the PSD [H] as the aerosol particles take up water and grow in size. A growth factor can be calculated based on the dry aerosol volume of the chemical composition measurements and the added volume of water as calculated by ISORROPIA. The new PSD can then be calculated with help of the aerosol growth factor. The chemical composition of the aerosol mixture is complemented with water, as the aerosol particles are no longer dry [F]. The resulting refractive index [G] can be calculated based on this chemical composition.

Output: Scattering coefficient

The Mie-model [I], another existing model that is used in the H-model, calculates the scattering and extinction values [J] based on the enhanced PSD and refractive index of the aerosol particles. To calculate the enhancement factor [J], a series of calculations can be made with a range of RH as input, resulting in a range of scattering and extinction values depending on the RH.

The H-model is based on existing models such as the MIE-model and ISORROPIA. The added value of the H-model, is the integrated calculation of scattering properties of aerosol compositions at different RH values. The H-model makes sure the input and output variables of both models are connected and calculated, so that the scattering properties can be calculated based on the H-model input variables.

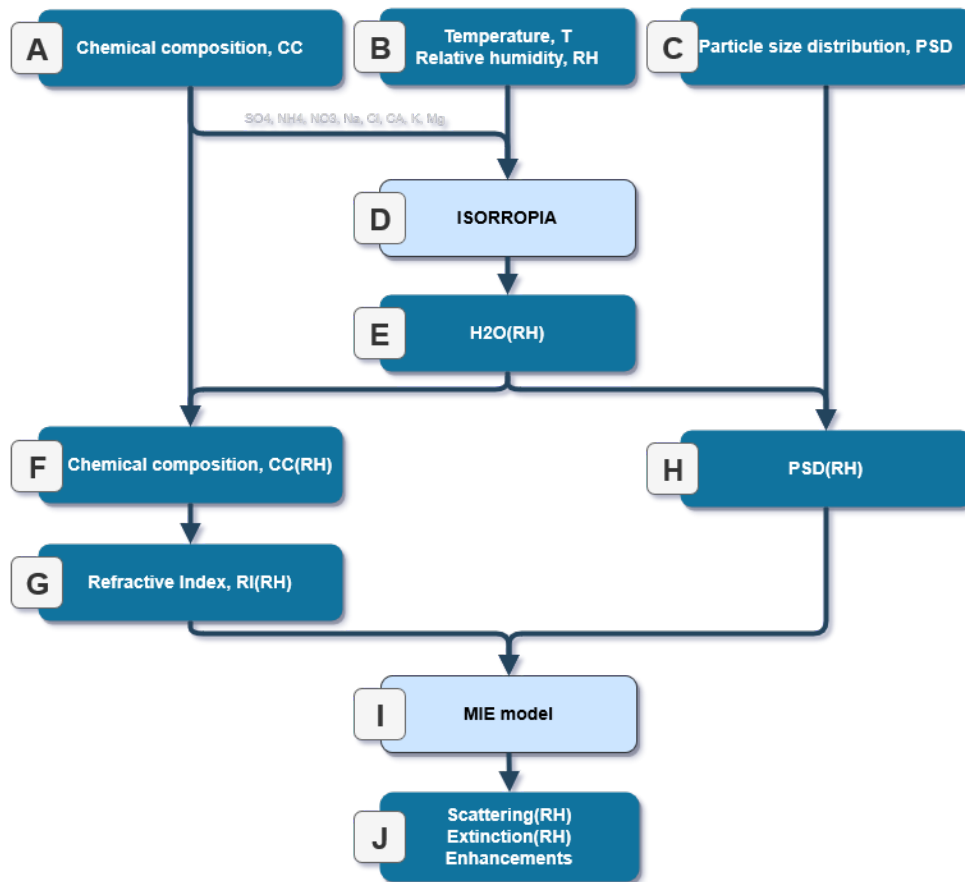


Figure 3.1: Components and steps of the H-model for calculating scattering properties based on in situ measurements.

3.2 Sub-models used in the H-model

3.2.1 ISORROPIA [D]

ISORROPIA is a thermodynamic equilibrium model that focuses on the ammonia-sulfate-nitrate-chloride-sodium-calcium-potassium-magnesium-water inorganic aerosol system (Fountoukis and Nenes, 2007). The H-model uses ISORROPIA Version 2.1 (07/19/09). As input, the model requires the mass concentration of ammonia, sulfate, nitrate, chloride, sodium, calcium, potassium, and magnesium and a given temperature and relative humidity. Based on this input, ISORROPIA estimates the concentrations of different aerosol species, as well as the composition and the phase state. One of the output variables is the amount of liquid water which is present in the aerosol system. This output variable will be used in the H-model. The other output variables, which are not used in the H-model, make it possible to analyze possible reasons of the hygroscopicity of certain compositions, if needed.

Using ISORROPIA we calculate the amount of water based on the input aerosols which only consist of Sea Salts (SS) and Secondary Inorganic Aerosols (SIA). These aerosol capture the bulk of the hygroscopic behaviour, but it has to be mentioned that in this specific model we ignore possible small hygroscopic behaviour of other aerosol species such as organics.

Settings

To run the ISORROPIA model, the setup configuration to describe the possible states of the aerosols has to be selected. It is possible to run the model with aerosol particles that contain:

- [1] solid as well as liquid phases (thermodynamically stable state)
- [2] only liquid state (meta stable state).

To imitate ambient conditions, it would be more realistic to select the meta stable state. Ambient conditions (in the Netherlands) generally have a relative high RH, so it can be safely assumed that the particles are only in their liquid state.

If the output of ISORROPIA is used to calculate scattering properties which will be compared to the measurements of the humidified nephelometer (WetNeph), the chosen setting should depend on the measuring method of the WetNeph. Whenever the WetNeph measures a full RH-cycle, often the RH of the ambient air is first dried (<40%) and then enhanced to higher RH values. In that case one should assume solid as well as liquid phases of the aerosol particles, so it is advised to use the thermodynamically stable setting. However, if the WetNeph does only enhance the ambient air or only measures air with a high RH, the meta stable state should be used, because the particles will be expected to stay in their liquid state. In this study the calculations of the CINDI campaign are executed in the thermodynamically stable state as the WetNeph did measure a full RH cycle. The calculations of the TROLIX campaign should be executed in the meta stable state as the WetNeph did only measure at enhanced RH (RH≈85%).

3.2.2 Mie model [I]

Mie lognormal model

The 'MEERHOFF MIE PROGRAM version 3.0' is used to calculate the scattering properties for the particle size distribution. The Meerhoff Mie program was developed at the Free University of Amsterdam, Physics and Astronomy Department. The calculations within the 'MEERHOFF MIE PROGRAM' are made according to the Mie theory as documented by De Rooij and Van der Stap (1987). It calculates, amongst others, the scattering coefficient (σ_s), the extinction coefficient (σ_e), the geometrical cross section (G), Scattering efficiency (Q_s) and Extinction efficiency (Q_e). The MIE model can calculate these values for a single aerosol particle but also for a lognormal distribution, which is the used approach in the H-model. As input variables, the used model requires a lognormal distribution (described by a geometric mean (μ_g) and standard deviation (σ_g)) of the aerosol particle size distribution and refractive index of the aerosol mixture.

Mie-sizedis model

An estimated lognormal distribution of aerosols does not reflect the reality of the real PSD in ambient conditions, which is more complex. Using accurate measurements, it is possible to create a more realistic PSD. To be able to

calculate the scattering and extinction values for this more realistic PSD, the original Mie model, which only accepts lognormal distributions as input, is adjusted. This adjusted Mie model is called the Mie-sizedis model and is provided by TNO.

The Mie-sizedis model calculates the scattering properties separately for 100 bins of the PSD and combines the results afterwards. To do so, the measured PSD needs to be split into 100 logarithmic bins from $D=0.01$ to $D=10\mu\text{m}$ before it is given as input to the Mie-sizedis model (Figure 3.2). Every bin is represented by a small lognormal distribution to calculate the scattering properties. The small lognormal distribution that represents the bin has a geometric standard deviation (σ_g) of $1.05\mu\text{m}$, regardless the bin diameter, and a geometric mean (μ_g) corresponding to the location of the bin itself (D_i [μm]). The Mie-sizedis model calculates the scattering coefficient for every representative bin. The total scattering coefficient of the entire PSD can then be calculated as follows:

$$\sigma_{total} = \sum_{i=1}^{100} \sigma_i \cdot N_i \quad (3.1)$$

where i is the bin number, σ_i the scattering coefficient for a lognormal distribution with $\mu_g = D_i$ and $\sigma_g = 1.05$ and N_i is the number of aerosols per bin. As a result, one value for the scattering and extinction coefficient can be found that represents the entire PSD. This approach is tested by comparing a simple lognormal distribution to the same lognormal distribution, but divided into 100 bins. The outcome falls within a 2% range of each other. So, the 'MIE-sizedis model' calculates the scattering properties for a particle size distribution which is better adjusted for a PSD that does not have to have the shape of an lognormal distribution.

An addition to the Mie-sizedis model is made by including the calculated geometrical cross section (G) and Scattering efficiency (Q_s) of the PSD in order to visualize the different contributions of these two variables to the scattering coefficient. The variables are calculated as follows:

$$G_{total} = \sum_{i=1}^{100} G_i \cdot N_i \quad (3.2)$$

$$Q_{s,total} = \sum_{i=1}^{100} Q_{s,i} \cdot \frac{G_i \cdot N_i}{G_{total}} \quad (3.3)$$

where G_i is the average geometrical cross section per bin and $Q_{s,i}$ is the average scattering efficiency per bin.

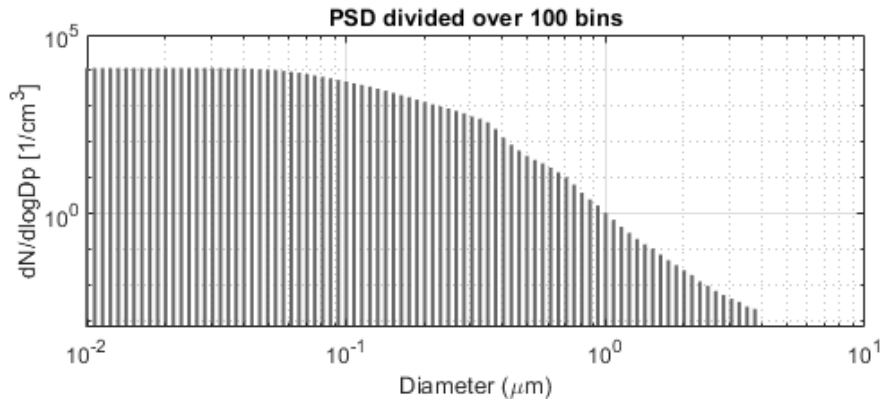


Figure 3.2: PSD divided into 100 log-scale bins.

3.3 Input/Output variables

The different model steps are visualized in Figure 3.1. Below, the different input and output variables of the remaining steps are explored and explained to create an understanding of the model and all of its aspects. Assumptions will be described in order to interpret the model output values correctly. This study focuses on all particles with a diameter smaller than $10 \mu\text{m}$ ($D_p \leq 10 \mu\text{m} = \text{PM}_{10}$).

3.3.1 Chemical composition (dry) [A]

The chemical composition of the aerosol particles is one of the three input variables of the H-model. In this study it is assumed that all aerosols, small or large, have the same chemical composition. The chemical composition is required to estimate the refractive index and to give input to ISORROPIA to estimate the liquid water content of the aerosols. The measurement of the chemical composition is divided into subgroups: Secondary Inorganic aerosols (SIA), Elemental carbon (EC), Organic Carbon (OC), Sea Salt (SS), and other (remaining metals, minerals, etc.). Table 3.1 gives a short explanation on every aerosol species that is used as input for the H-model and certain measuring instruments that are used during this study.

Chemical composition changes spatially and temporally. High temporal measurements of the chemical composition are preferred as this leads to more accurate comparisons. Average daily values give a good first indication, but daily fluctuations of secondary aerosols will be lost. If possible, a higher temporal resolution (multiple measurements a day) would be preferred. SIA, EC, OC, SS, metals and minerals can be measured by analyzing filters. The temporal resolution of these filters depend on the measured aerosol type but can be several hours or longer. Daily mean values are easily measured by filters. To measure with a higher temporal resolution it is possible, for example, to use a MARGA (Monitor for AeRosols and Gases in ambient Air) to measure SIA and SS concentrations. To determine EC (at higher resolution compared to filter measurements) it is possible to measure the amount of Black carbon (BC) in the air using a MAAP (Multi-Angle Absorption Photometer) and using these diurnal fluctuations to convert daily EC measurements to, for example, hourly measurements.

Table 3.1: Basic information on measured aerosols species needed as input for the H-model.

Aerosol species	Explanation
SIA	Sulfate (SO_4), ammonium (NH_4) and nitrate (NO_3) are the dominant species in secondary inorganic aerosols. Common ways to measure their mass concentrations are to load QMA-filters and using GC-MS (Gas Chromatography Mass Spectrometry) as analysis method or using MARGA measurements.
OC	The concentration of organic carbon (OC) can be measured by using EC/OC measurements. Organic carbon can be measured and can give a good approximation for (secondary) Organic Aerosol (SOA).
EC	EC concentrations can be measured with OC/EC filters. Another way to estimate EC is by measuring the amount of Black carbon (BC) in the air with the MAAP, which is an approximation of the EC mass concentration.
SS	Most important Sea Salts in the air are Sodium (Na), Chloride (Cl), Calcium (Ca), Potassium (K) and Magnesium (Mg). Common ways to measure SS mass concentration are (Teflon and QMA) filters or MARGA measurements. Depending on the type of measurements taken, it is not always possible to measure all SS components. Sometimes only Sodium is measured. The remaining unknown salt fractions can be estimated based on the salt fractions of the composition of SS in the sea itself. Atmospheric transformation, such that lead to e.g. a 'chloride deficit', are often ignored, but can be taken into account. The used salt fractions can be found in Table 3.2.
Other	Other particles such as metals and minerals form the remaining part. A common way to measure these concentration is by using Teflon filters.

Table 3.2: Composition of sea salt; based on seawater composition and ignoring atmospheric transformation (Seinfeld and Pandis, 2006).

Element	Percent by weight
Cl	55.04
Na	30.61
Mg	3.69
Ca	1.16
K	1.1
Remaining	8.4

3.3.2 Temperature and Relative Humidity [B]

The temperature (T) and Relative Humidity (RH) are input variables for the ISORROPIA model and indirectly affect the extinction, scattering and enhancement factor of the aerosols.

The input temperature and RH need to match with the conditions for which the H-model needs to be calculated the scattering properties. If the H-model were to be used for calculations of ambient conditions, then the ambient temperature and RH need to be selected. However, in this study the temperature and RH as measured in the nephelometer are used in order to make a correct comparison between the calculated and measured scattering coefficients.

3.3.3 Particle Size distribution (dry) [C]

The particle size distribution (PSD) is the last input variable needed for the H-model. During this study the PSD is measured using a Scanning Mobility Particle Sizer (SMPS) and an Aerodynamic Particle Sizer (APS). Both instruments measure the number of aerosols particles, but both have a different diameter size domain. Together they can measure a PSD between $D \approx 0.01 - 10 \mu m$ (See Figure 3.3). To avoid confusion and to easily compare multiple PSD data sets with different diameter resolutions, all data sets are also converted from number concentrations N to normalized concentrations $dN/d\log(D_p)$.

$$\frac{dN}{d\log(D_p)} = \frac{dN}{\log(D_{p,\text{upper limit}}) - \log(D_{p,\text{lower limit}})} \quad (3.4)$$

The APS measures the aerodynamic diameter (D_a) which has to be changed to physical diameters (D_p) in order to merge both data sets. In this study, it is assumed that all particles are spherical. Under this assumption, the aerodynamic diameters can be converted to physical diameters using the following relationship:

$$D_p = D_a \cdot (1/\rho_{eff})^{1/2} \quad (3.5)$$

With ρ_{eff} the effective density of the APS aerosols.

In this study, the SMPS and APS do not measure particle diameters in an overlapping region. To merge both data sets, it is chosen to (visually) align the particle number distributions. To do so, a value for ρ_{eff} is chosen such that the average values of the APS PSD and SMPS PSD seemed to be aligned optimally to the eye. For each campaign, one fixed value was chosen to represent the ρ_{eff} of all APS measurements. Once the ρ_{eff} is chosen, a fit is made through the merged data set so that the merged PSD can be divided into 100 bins (Figure 3.3).

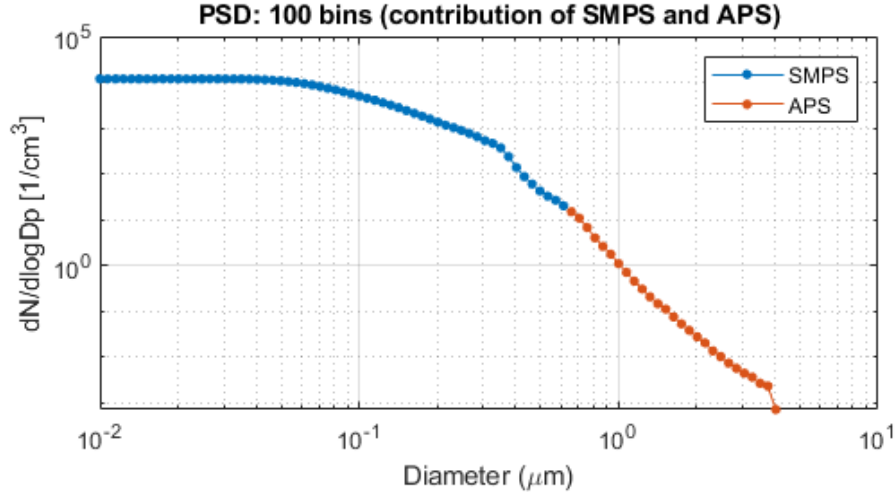


Figure 3.3: Example of the PSD based on SMPS and APS measurements after merging both data sets, divided into 100 log-scale bins.

3.3.4 Refractive index [G]

Based on the chemical composition of the aerosol, an average refractive index can be estimated which is needed as input for the MIE-model. It is assumed that all aerosol particles have the same chemical composition independent of the size of the aerosol, so one average value of the refractive index is taken to represent all aerosols. Different types of aerosol species will be distinguished, which all have their own refractive index (Table 3.3). The RI of OC and BC are also used as RI for Organic Matter (OM) and Elemental Carbon (EC), respectively. 'Other' aerosol species from Table 3.1 are not taken into account as they are just a small part of the entire aerosol volume composition and a clear value for the refractive index is missing.

To determine an overall refractive index (RI), a volume-weighted approach is needed. The volume per species is based on the measured mass concentration and the mean species density.

$$RI_{total} = \frac{V_{SS} \cdot RI_{SS} + V_{SIA} \cdot RI_{SIA} + V_{OA} \cdot RI_{OA} + V_{EC} \cdot RI_{EC} + V_{H_2O(RH)} \cdot RI_{H_2O}}{V_{Total}(RH)} \quad (3.6)$$

with V_{total} :

$$V_{Total} = V_{SS} + V_{SIA} + V_{OA} + V_{EC} + V_{H_2O(RH)} \quad (3.7)$$

The volume mixing method from Equation 3.6 is used for the real part as well as the imaginary part of the refractive index. As can be seen in the formula, the RI will change with varying RH and thus water. Water has a lower value for its refractive index than the other aerosol species, so the RI decreases as the RH approaches 100% and the amount of water increases.

Table 3.3: Refractive index of different aerosol composition ($\lambda \approx 550nm$) ((Kim et al., 2015),(Seinfeld and Pandis, 2006), (Shettle and Fenn, 1979), (Hess et al., 1998))

-	RI (R)	RI (I)
SS	1.5	$1 \cdot 10^{-8}$
SIA	1.53	$6 \cdot 10^{-3}$
OC	1.47	$4 \cdot 10^{-2}$
BC	1.75	$4.4 \cdot 10^{-1}$
Water	1.333	$1.96 \cdot 10^{-9}$

3.3.5 Particle size distribution (wet) [H]

Due to the water uptake of the aerosol particles at a given RH, the particles will grow in volume. To calculate the new enhanced PSD, the growth factor is needed. It is possible to calculate the hygroscopic volume growth factor $g_v(RH)$ (Equation 3.8) or (diameter) growth factor $g_D(RH)$ (Equation 3.9). The growth factor expresses the (average) growth of an aerosol for a given RH compared to the dry-aerosol volume or diameter, due to hygroscopic behaviour.

$$g_v(RH) = \frac{V_{\text{total, aerosol}}(RH)}{V_{\text{total, aerosol}}(RH = Dry)} \quad (3.8)$$

$$g_D(RH) = \frac{\text{Diameter}_{\text{aerosol}}(RH)}{\text{Diameter}_{\text{aerosol}}(RH = Dry)} \quad (3.9)$$

$V_{\text{total, aerosol}}(RH = dry)$ is the total aerosol volume based on the measurements of the dry chemical composition. $V_{\text{total, aerosol}}(RH)$ is the total aerosol volume based on the measurements of the chemical composition and the total water volume as calculated by ISORROPIA at a certain RH. When the growth factor $g(RH)$ is discussed in literature, it often refers to the diameter growth factor $g_D(RH)$. Both factors are shown here as the volume growth factor is needed for the ISORROPIA approach and the diameter growth factor is needed for the k-Köhler approach which will be discussed later in this study as well. The relation between both factors is as follows:

$$g_D(RH) = g_v(RH)^{1/3} \quad (3.10)$$

It is assumed that all aerosol particles have the same chemical composition independent of the size of the aerosol, this is why the assumption is made that all aerosols, small or large, will grow with the same growth factor. To simplify the situation, it will be neglected that the size of the particle influences the degree of hygroscopicity. Figure 3.4 shows an example of a growing PSD due to increasing RH, under these assumption.

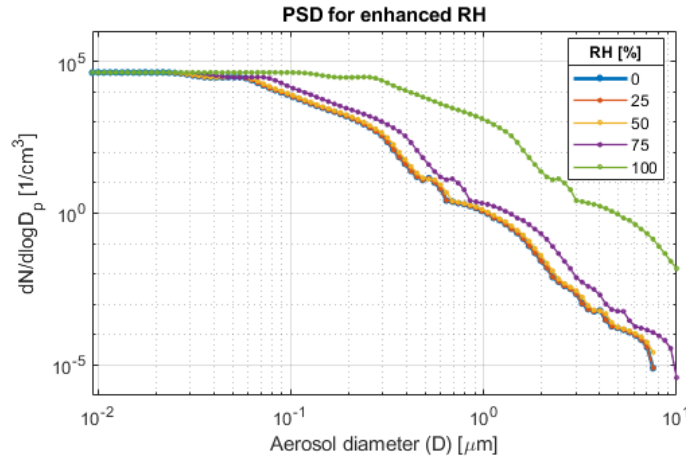


Figure 3.4: Example PSD for different values of RH based on total-volume growth. The PSD of RH=0 and RH=25 are overlapping.

3.3.6 Enhancement factors [J]

Next to the scattering and extinction coefficients the enhancement factor $f(RH)$ as described in Equation 2.5 can be calculated. To do so, the H-model results of the scattering coefficients at different values of RH can be used.

4 Model validation

To validate the H-model, the calculated scattering coefficients and enhancement factors have been compared to values measured by the WetNeph. The WetNeph is a humidified Nephelometer which directly measures the scattering coefficient at specific wavelengths. The WetNeph can humidify or dry the ambient air and can therefore also measure the scattering values at enhanced RH to calculate the enhancement factors. The scattering values of the H-model can thus be compared to the scattering values from the WetNeph. To distinguish between the scattering coefficients which are calculated by the H-model and the scattering coefficients measured by the nephelometer, they will be referred to as 'calculated (model) values' and 'measured (WetNeph) values' respectively.

The validation of the H-model is done in 3 different steps. Validating the entire H-model is first done with data from the CINDI (Cabauw Intercomparison of Nitrogen Dioxide measuring Instruments) campaign in 2009 at Cabauw (section 4.1). Subsequently, based on the CINDI results a sensitivity analysis to better understand specific aspects of the model (section 4.2) is performed. In addition the H-model is validated with new measurements made during this study in September 2019 (section 4.3) during the TROLIX (TROpomi vaLIdation eXperiment) campaign, also at Cabauw.

During this study, a wavelength of 550 nm is used for all the comparisons and calculations concerning scattering properties. This wavelength is around the peak of the visible light spectrum and is a commonly used wavelength amongst instruments measuring light scattering. 550 nm is also one of the specific wavelengths used by the nephelometer.

4.1 Model test run and comparison with measurements from the CINDI campaign

During the CINDI campaign in 2009, different variables concerning scattering properties were measured at the CESAR (Cabauw Experimental Site for Atmospheric Research) site. Most importantly, a humidified nephelometer was used to measure scattering and extinction values at different RH-values. Temperature and RH was continuously measured at Cabauw and also the PSD was measured during the same period. The used data to calculate the scattering values is described below. The data from 4 to 19 July is used, as this was the period with sufficient overlapping data of all measuring instruments for a first test run of the model. The temporal resolution of the WetNeph is 3 hours when measuring enhancement factors. All other input variables are scaled to average values of 3 hours.

4.1.1 Input data

Nephelometer

The WetNeph which was used during the CINDI campaign has measured scattering coefficients and corresponding enhancement factors. To determine the enhancement factors, the air supply to the nephelometer is dried and enhanced so that the scattering coefficients and thus enhancement factors can be calculated at different values of RH. However, in the first week of the campaign (5 to 12 July), the relative humidity was kept constant, so during these days there are no measured enhancement factors. This data has been provided by Paul Zieger [ACES, Stockholm University]. For the purpose of validating the H-model, this study uses the enhancement factors $f(\text{RH}=85\%)$ for the wavelength $\lambda = 550\text{nm}$.

Particle size distribution

The aerosol size distribution is measured by an SMPS and APS. Both distributions are combined assuming a ρ_{eff} of 2g/cm^3 . During the entire research period, the SMPS did not work properly for small diameters, as illustrated by the measured size distribution shown in Figure 4.1a: The PSD should not decrease in number concentration for aerosols with a diameter below approximately $0.04\ \mu\text{m}$, the measurements of the SMPS at small diameters are therefore not correct (J.S. Henzing, personal communication, 2019). To improve the data set, the decrease

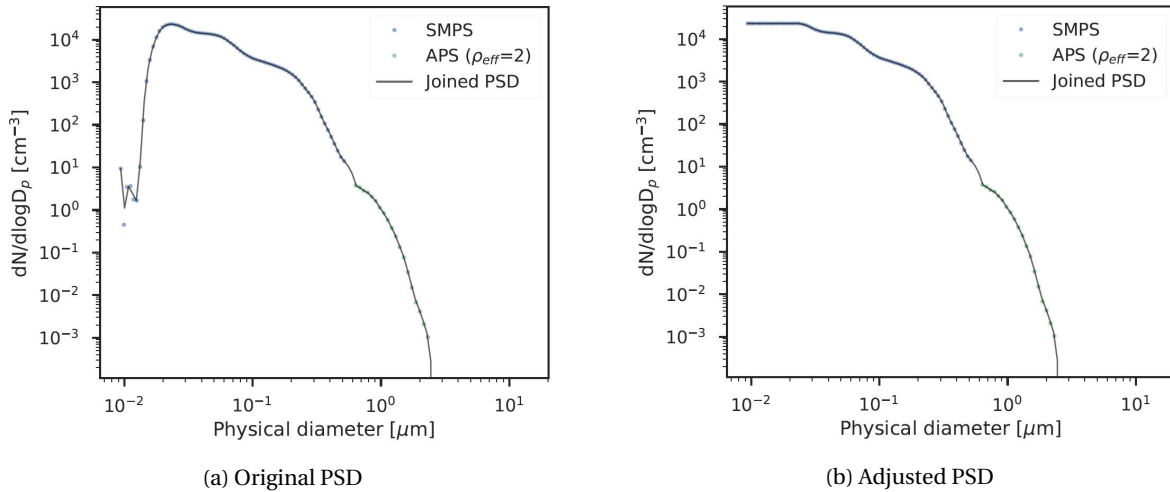


Figure 4.1: Example of a combined PSD from the SMPS and APS (left: original, right: adjusted).

in number concentration at small diameters is ignored and it is assumed that the number concentration does not decrease for particles with a diameter up to $0.04 \mu\text{m}$. A corrected PSD to account for that is shown in Figure 4.1b and can be compared to Figure 4.1a. Although this adjustment is an improvement of the original PSD, it will never be the exact representation of the true PSD. Fortunately, particles with such small diameters have a negligible influence on the scattering properties. This is due to the scattering efficiency that decreases exponentially for small aerosol particles.

Chemical composition

The chemical composition of the aerosols in the CINDI data set turned out to be incomplete, as only a few aerosol species were measured directly at Cabauw during the CINDI campaign. To estimate missing species of the chemical composition at the site, the LOTUS-EUROS model is used.

LOTUS-EUROS is an open-source chemical transport model developed at TNO which estimates specific gas and aerosol concentrations based on atmospheric transport, chemistry, deposition and emissions. The data has been provided by existing data sets from 2009 by TNO. The spatial resolution of this LOTOS-EUROS run is 7 by 9 km. The output for the Cabauw location is merely used as an approximation of the true concentrations. Most concentrations are described in fine ($D_p \leq 2.5 \mu\text{m}$) and course ($2.5 > D_p \leq 10 \mu\text{m}$) mode. In this study no difference is made between the chemical composition of small and large particles, so both outputs are combined to result into a aerosol species concentration of $D_p \leq 10 \mu\text{m}$.

Some aerosol species were measured during the research period, others have been estimated using the LOTOS-EUROS model. Table 4.1 provides an overview of all the aerosol species that are input values for the H-model during the test run. The table describes the measurements that are used for each aerosol species. The estimated aerosol volume based on the chemical composition is scaled to match with the measured volume of the PSD.

Table 4.1: Basic information on estimated aerosols species as measured or assumed during the CINDI campaign 2009.

Aerosol species	Measurement technique and assumptions
SIA	LOTOS-EUROS gives an estimation of the mass concentration of Secondary inorganic aerosols (SIA), in this case sulfate (SO ₄), ammonium (NH ₄) and nitrate (NO ₃).
OC	The concentration of organic carbon (OC) was not measured or calculated. A rough estimation is made by assuming a diurnal cycle with an average minimum of 1 $\mu\text{g}/\text{m}^3$ and a maximum of 2 $\mu\text{g}/\text{m}^3$. The concentration is modelled as a daily sine wave with its minimum and maximum peak correlating with the concentration of the nitrate concentration (maximum peak during night). For this test run, the OC concentration is assumed to be equal to the ambient SOA concentration.
EC	Due to the measurements of the MAAP (Multi-angle absorption photometer) the concentration of black carbon (BC) can be estimated. The MAAP measures the aerosol absorption coefficient at a wavelength of +/- 637 nm. BC is the prime absorber in this region of the solar spectrum. To convert from the absorption coefficient to BC mass concentration, the Mass Absorption Coefficient (MAC) is used. For this test run the BC concentration is assumed to be equal to the ambient EC concentration.
SS	From all the Sea Salts, LOTOS EUROS only predicts Sodium (Na). The remaining unknown salt fractions are estimated based on the salt fractions of the composition of sea salt using Table 3.2 (Seinfeld and Pandis, 2006);
Other	Remaining metals and minerals are not taken into account during this trial run.

4.1.2 Results from the CINDI campaign

Figure 4.2 shows the scattering enhancement factor $f(\text{RH})$ at $\text{RH}=85\%$ during the period of the campaign. It compares $f(\text{RH}=85)$ values calculated by the H-model with the measurements by the WetNeph. The H-model clearly calculates larger enhancement factors than the measured outcome by the WetNeph. According to general WetNeph measurements, the scattering enhancement at Cabauw has a mean of 2.38 (std=0.38), so enhancement factors rarely exceed an enhancement factor 4 (Zieger et al., 2013). The output of H-model is thus apparently too large with values ranging from 2 up to 11. In addition, Figure 4.3 visualizes the $f(\text{RH})$ dependence as a function of RH for all measured data points calculated by the H-model. The mean scattering enhancement can be easily read from this graph, and for $\text{RH}=85\%$ it is approximately 5.4. The peak which can be seen at $\text{RH}=30\%$ is unexpected, but does not apply to all measurements.

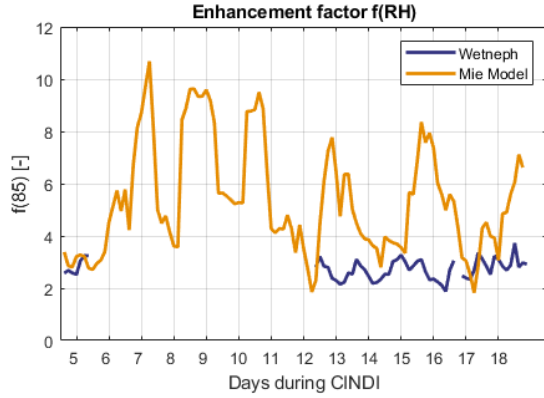


Figure 4.2: Enhancement factor $f(\text{RH}=85)$ ($\lambda = 550\text{nm}$) measured by the WetNeph and calculated by the H-model during the campaign.

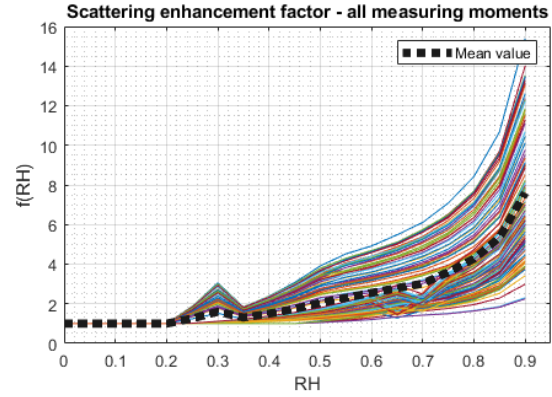


Figure 4.3: Collection of all $f(\text{RH})$ calculations by the H-model ($\lambda = 550\text{nm}$).

The calculated enhancement factors are too large and are probably caused by the large concentration of hygroscopic particles. The hygroscopicity of the aerosol mixture is too large and mainly caused by the concentration of Sea Salt particles and the large ratio of the Sea Salt mass concentration to the remaining aerosol mass concentration. Figure 4.4 visualizes the correlation between the different aerosol species with respect to the enhancement factor of $\text{RH}=85\%$. It can be clearly seen that the amount of SS correlate with the $f(\text{RH})$. A simple test on linear relationship shows that the mass fraction of SS has a positive and stronger correlation ($R = 0.97$) to the enhancement factor, this compared to SIA ($R = -0.80$), SOA ($R = -0.48$) and BC ($R = -0.70$).

Figure 4.5 visualizes the scaled mass concentration of all aerosol species used as input for all measurements during this first model run. The mean mass concentration of SS is $2.8 \mu\text{g}/\text{m}^3$ and maximum values are about $6.9 \mu\text{g}/\text{m}^3$. In the Netherlands, the mean of daily average concentrations varies between $2\text{-}4 \mu\text{g}/\text{m}^3$ and the maximum daily average concentrations varies between $10\text{-}15 \mu\text{g}/\text{m}^3$, with highest values near the coastlines (Manders et al., 2009). Although the SS concentration strongly affects the enhancement factor, the used mass concentration of sea salt in the atmosphere is reasonable, so the absolute quantity of the SS particles is not expected to be the reason for the overestimation of $f(\text{RH})$. But, the main reason for the over estimation of $f(\text{RH})$ is probably due to the fraction of SS in the aerosol. Figure 4.5 shows that the mass concentration of Sea Salt is often more than 50% of the total aerosol concentration which is unrealistic for aerosols in the Netherlands. As shown by Manders et al. (2009) the sea salt typically contributes between 5 and 50% to PM_{10} . And for low aerosol concentrations (Total aerosol $< 30 \mu\text{g}/\text{m}^3$), such as in our measurements, the average SS concentration is about 16% according to Buijsman et al. (2013). The large hygroscopicity of Sea Salt particles in combination with the (too) high ratio of Sea Salt particles, is probably the reason for an overestimation of the enhancement factor in this test run.

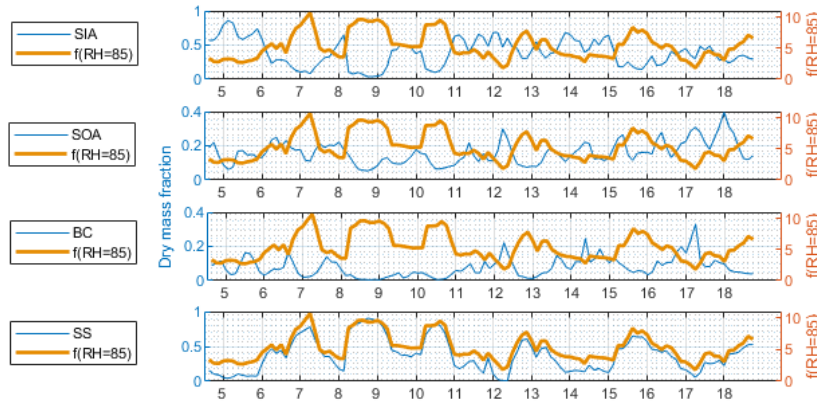


Figure 4.4: Mass concentration of different aerosol species at all measuring moments compared to the final enhancement factor $f(\text{RH}=85)$ ($\lambda = 550\text{nm}$).

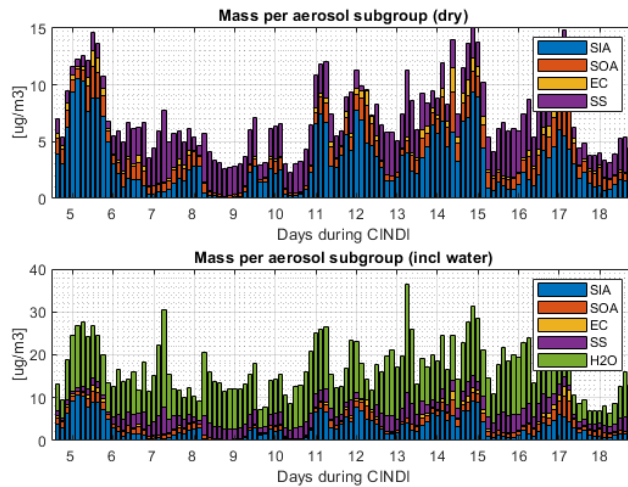


Figure 4.5: Mass concentration of different aerosol species at all measuring moments.

Using the CINDI dataset as input for the H-model provides a first insight into the working principles of the H-model. Evidently the model gives some reasonable results. Depending on the aerosol chemical compositions and PSD, the model can calculate enhancement factors based on the hygroscopicity and refractive index of the aerosol composition. However, it seemed that with the current H-model and with the current input values, the output is not yet realistic. It can be concluded that the input values, in particular the relative ratios, of the chemical composition are not complete or realistic. By combining measurements with models (LOTUS-EUROS) and partly due to rough assumptions, the overall chemical input seems inaccurate. This is why a more complete data set from another measurement campaign is needed. A new measurement campaign of multiple weeks is discussed in section 4.3. Furthermore, the H-model itself shows some surprising results as well, such as large scattering values at low and high RH (Figure 4.3). This warrants a sensitivity analysis of the model, which is discussed first in section 4.2.

4.2 Sensitivity analysis

ISORROPIA is a vital part of the H-model as it directly influences the particle volume growth ($g_v(RH)$) by calculating the amount of water in the aerosol composition. ISORROPIA itself is not explained in detail in this study as it is mainly used as a black-box. Nevertheless, by analyzing results of ISORROPIA based on different input values, a better insight in its working principle will be provided. The test run of the enhancement factor shows some unexpected behaviour, such as significant scattering enhancement at low RH values. By performing a sensitivity analysis a better understanding of the different aerosols species and their effect on the particle hygroscopic growth is investigated.

4.2.1 ISORROPIA-aerosol species combinations

The standard chemical input of ISORROPIA consists of SS and SIA. The first sensitivity test investigates the relative importance of these two species. In this sub-study a particle size distribution (chosen from the CINDI data) with a total dry aerosol volume of $4.3 \times 10^6 \mu\text{m}^3$ per cubic meter air is used. Three different chemical mixtures were considered to calculate the effect of the water-uptake, the growth-factor and its effect on the enhancement factor. The 3 mixtures which are analyzed are as follows:

1. The aerosol particles are a Na-Cl-Ca-K-Mg salt mixture (SS-mixture). The densities of the salts are assumed to be the same ($\rho = 2.17 \text{ g/cm}^3$) and the amount of each specific salt is based on the salt ratios found in Table 3.2.
2. The aerosol particles are a NaCl (Na-Cl mixture). A density of $\rho = 2.17 \text{ g/cm}^3$ is used.
3. The aerosol particles are a SO₄-NH₄-NO₃ mixture (SIA mixture). A density of $\rho = 1.76 \text{ g/cm}^3$ is used.

The SS and SIA mixture are chosen to represent both aerosol species. In addition it was chosen to analyze a mixture solely using NaCl particles as this is a combination often used in literature, so a simple check can be done to see if the ISORROPIA model predicts credible values. The three different mixtures are put into ISORROPIA with a constant temperature of 293 K and different values of RH (between 0-100, with steps of RH=5). The volume and diameter growth factor is calculated for every RH-step using Equation 3.8 and 3.9 and the estimated amount of liquid water.

Figure 4.6 shows the calculated growth factor for each RH-step. The Na-Cl mixture seems to take up water according to theory, having a deliquescence point between 70-80% and a diameter growth factor of approximately 2 at RH=80% (Pinterich et al., 2017). The growth of the SIA mixtures also agrees with the general behaviour of inorganic aerosols, having a diameter growth of 1.5 at RH=80% (Wise et al., 2003; Latimer and Martin, 2019). The growth factor of the Na-Cl-Ca-K-Mg salt mixture starts to increase at a much lower RH than expected for salt particles in the ambient air. This is caused by ion combinations that have a low deliquescent point such as CaCl_2 or MgCl_2 which have a hygroscopic growth that starts already at low RH values (Guo et al., 2019). In addition, the sudden volume growth followed by a volume decrease near RH=30%, which was also seen in the first model runs in Figure 4.3, is visible in the Na-Cl-Ca-K-Mg salt mixture as well. The decrease in growth factor is due to a change in ion combinations at different RH values. Near a RH of 30 %, ISORROPIA predicts a lot of change in the ion combinations, which makes it hard to pinpoint the exact changes responsible for this short decrease in growth factor.

Figure 4.7 visualizes the scattering enhancement factor $f(RH)$ based on the three input mixtures and their growth factors. At a relative humidity of 85%, the enhancement factor is approximately 15, 11 and 4 for the Na-Cl-Ca-K-Mg, Na-Cl and SIA mixtures respectively. Values of $f(RH=85)$ should be around 2 for average aerosol conditions at Cabauw. Assuming that ISORROPIA works correctly, this suggests that a high concentration of low hygroscopicity aerosols is needed to reduce the overall growth-factor of the aerosols in order to make sure the enhancement factor will decrease as well. This could explain that the test run (Figure 4.2) has such high values for the enhancement factor, simply because the concentration of, for example, sea salt or SIA is too high with respect to other aerosol species (Figure 4.5). This confirms that the input variables from the test run are not realistic and new measurements are needed. Another explanation which partly could explain the large enhancement factors is the chosen set of ISORROPIA combinations of this sub-study. The possible combinations of the aerosols are limited. This is why the sensitivity study in subsection 4.2.2 is done to find out more about individual elements rather than aerosol species.

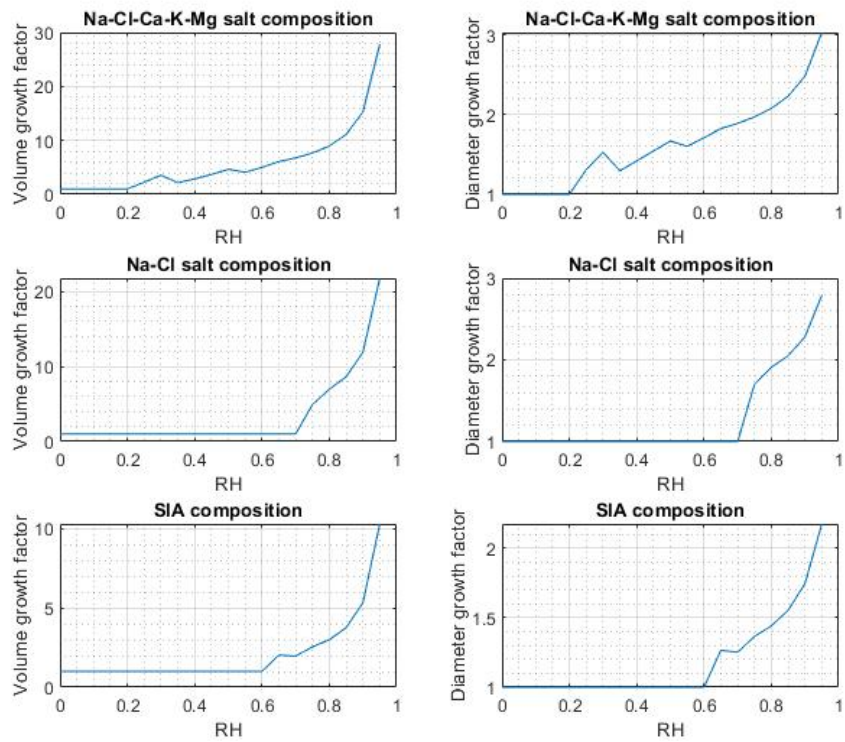


Figure 4.6: Volume and diameter growth factor as a function of RH as predicted by ISORROPIA.

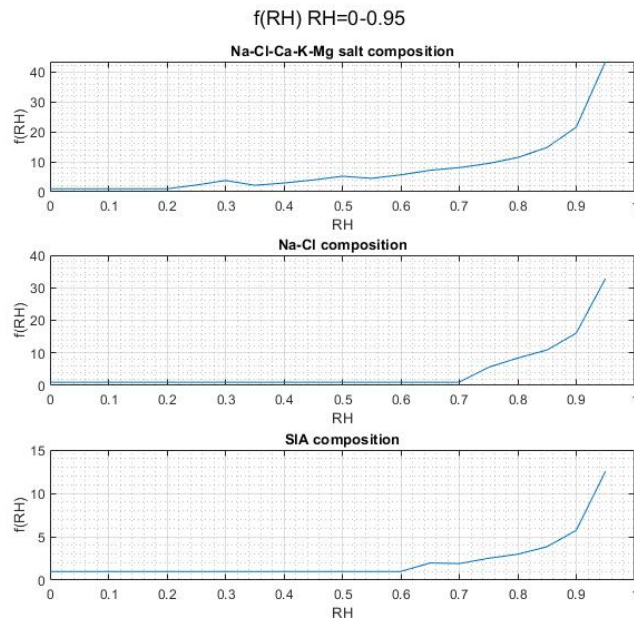


Figure 4.7: Enhancement factor ($\lambda = 550\text{nm}$) as a function of RH according to ISORROPIA sensitivit results in combination with the H-model.

4.2.2 Sensitivity of the ISORROPIA model

Following from the results from section 4.1 and subsection 4.2.1, a closer look at the different input aerosol elements and their effect on the growth factor and enhancement is required. To do so, a sensitivity study was carried out where a chemical mixture from the CINDI-campaign is used on a day when the $f(\text{RH}=85)$ has credible values (4-7-2009 18:00-21:00). It is thus assumed that the used ratios of the chemical composition are realistic input values. This chemical mixture is put into the H-model and run several times. Each run, one specific aerosol element is left out and the missing aerosol volume is filled with the remaining aerosol species (scaled). Figure 4.8 visualizes the amount of each aerosol species within the PSD for every run. The top bar graph shows the input quantities for the model. The bottom bar graph includes the amount of water which is calculated by the model to be part of the aerosols at an enhanced RH of 85%.

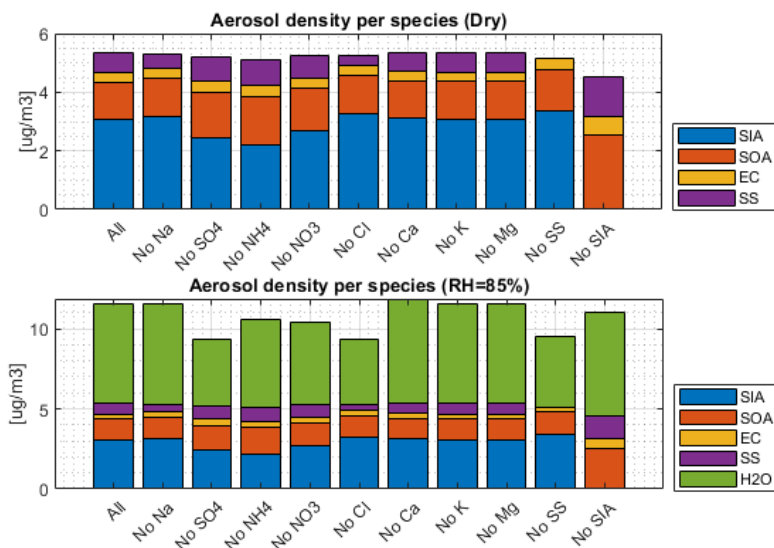


Figure 4.8: Variations of a chemical aerosol mixture with the same PSD (and same total volume). Top bar graph shows the dry chemical mixture. Bottom bar graph shows the chemical mixture at 85% relative humidity including water calculated by the model.

ISORROPIA thus estimates a different amount of liquid water for the different aerosol mixtures which results in a different growth factor and refractive index. For each mixture the enhancement factor $f(\text{RH})$ is calculated (Figure 4.9), which shows a large variability of $f(\text{RH})$ for the different runs. By removing only specific aerosol species from the mixture the enhancement factor at 85% changes between 2.2 and 3.3.

Another important realisation is that the increase of $f(\text{RH})$ starts at different values of RH for different aerosol mixtures. Aerosol mixtures without SO₄ or SIA (including SO₄) show an increase of $f(\text{RH})$ below 40% (Figure 4.9). This can be explained by a shortage of SO₄. Under normal conditions, Ca and Mg tend to combine with SO₄ particles as CaSO₄ and MgSO₄. Due to the absence (or a shortage of) SO₄ in the air, Ca and Mg will bind with Chloride particles and form CaCl₂ and MgCl₂ which have a much lower deliquescent point resulting in hygroscopic growth at low RH values. Possibly, standard ambient aerosol air conditions contain sufficient SO₄ particles to prevent this from happening.

From the sensitivity study, it can be concluded that not only the RH but also the exact chemical composition has a significant effect on the scattering and enhancement factors. ISORROPIA is sensitive to small changes in the chemical composition because it estimates the possible aerosol combinations based on the chemical input. All these different aerosol combinations have their own hygroscopic behaviour, affecting the growth factor and enhancement factor of the total aerosol mixture. This once again shows the importance of complete and accurate species measurements.

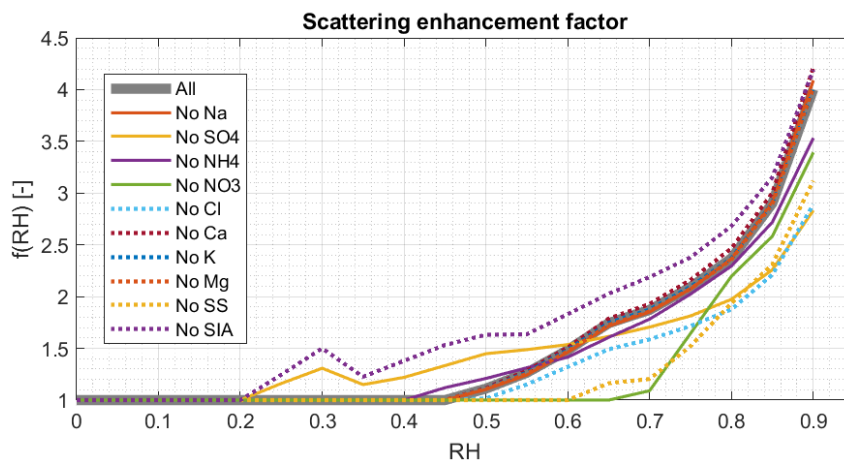


Figure 4.9: The enhancement factor ($\lambda = 550\text{nm}$) calculated by the model based on variations of a standard chemical mixture of aerosols with the same PSD.

4.3 Model run and comparison with measurements from the TROLIX campaign

During the TROLIX campaign in 2019 some measuring instruments were set up for this study in order to generate new input. Again, a validation attempt is made by comparing H-model results with measured data. Measurements of the chemical composition, optical properties and particle size distributions were taken at Cabauw between 10 September and 7 October 2019.

4.3.1 Input data

In order to validate the H-model, the calculated scattering values are compared to those measured by the nephelometers. During the first days of the campaign, the nephelometers were not yet ready to be used, and halfway during the campaign the water supply was interrupted so no RH enhancements could be measured. As a result, only 16 out of 28 days could be used for the validation. Table 4.2 visualizes for which exact period the comparison can be made. However, not all data of the TROLIX campaign was available in time to be included in this report. The focus is on the data between 14 and 23 September. For further research, the remaining 6 days can be included to better substantiate the results.

Table 4.2: During the TROLIX campaign, aerosol measurements were taken at Cabauw for 4 weeks. Days coloured in red have an incomplete data set, days coloured in dark green have a complete data set and are used in this study, days in light green have a complete data set which is not yet available.

September														October														
10	11	12	13	14	15	16	17	18	19	20	21	22	23	24	25	26	27	28	29	30	1	2	3	4	5	6	7	
X	X	X	X												X	X	X	X	X	X	X							X

Nephelometers

Two Nephelometers were located at Cabauw during the TROLIX campaign. Two setups were used, each using a different nephelometer. To distinguish the two setups, they will be called the dry-setup and the wet-setup. To distinguish both Nephelometers, they will be referred to as old and new Nephelometer. The dry-setup measures scattering values at a dry relative humidity ($\text{RH} < 40\%$), for this the ambient air will be dried. The wet-setup measures at high RH, for this the RH of the ambient air will be enhanced if needed. The scattering enhancement $f(\text{RH})$ can be calculated based on the different results of the dry and wet-setup. These results will be compared to the scattering enhancements calculated by the model. The humidified nephelometer tries to enhance the ambient air to a relative humidity of 85%. However the final RH fluctuates between 70 and 95% while trying to reach this value.

Particle size distribution

The aerosol size distribution is measured by an APS and SMPS. Similar to the measurements from the CINDI campaign, the SMPS has trouble measuring aerosols at small diameters ($D < 0.04 \mu\text{m}$). Again, the PSD of the SMPS is adjusted for small particle diameters (see Figure 4.1). To merge the APS with the SMPS data set a single value for ρ_{eff} is chosen for all measurements during the campaign. To merge both data sets smoothly, a ρ_{eff} of 2.4 g/cm^3 had to be assumed for the APS to prevent a large jump in the mean PSD. Note that this ρ_{eff} is relatively large but necessary to prevent a jump in the merged PSD. Figure 4.10 shows that for mean campaign values, a large $\rho_{eff} = 2.4 \text{ g/cm}^3$ fits better to the data than a more often used value of $\rho_{eff} = 2.0 \text{ g/cm}^3$.

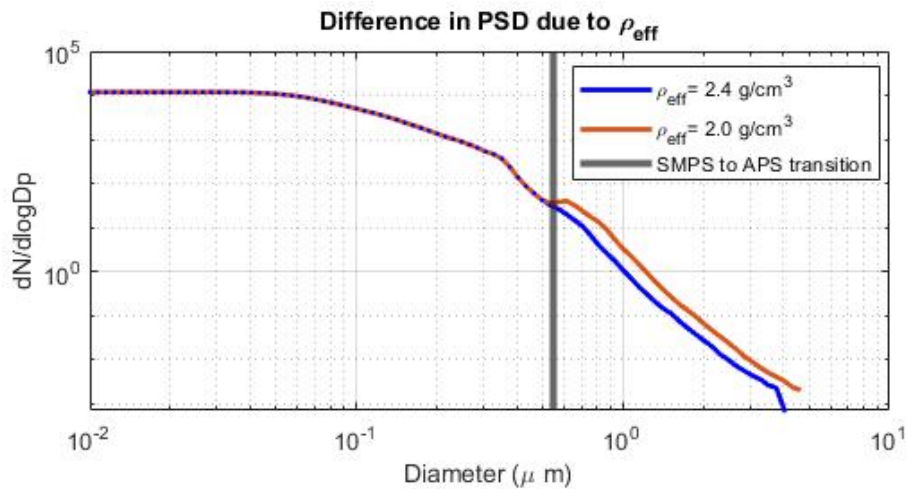


Figure 4.10: Mean PSD during the campaign based on the chosen ρ_{eff} .

Chemical composition

The chemical composition is measured by daily filters, except for the BC measurements by the MAAp. The daily measurements were taken from midnight to midnight, measured in Dutch winter time (UTC+1). Table 4.3 provides an overview of all the aerosol species that are input-values for the H-model during the TROLIX run. The table describes the measuring technique per aerosol species.

Temperature and relative humidity

The two nephelometers measure the scattering coefficients at different conditions compared to the ambient atmosphere. The RH is dried in the first setup and enhanced in the second setup. Due to the measuring techniques, the temperature within the instrument differs a lot from the temperature of the ambient air. Both setups measure the internal RH and temperature. These values are used as input for the H-model. Because the enhanced nephelometer (WetNeph) did not succeed in measuring at a constant value of $\text{RH}=85\%$, notice that as a result, the enhancement factor is not always $f(\text{RH}=85)$, but differs for every measurement. Most important is that the H-model calculates the enhanced scattering coefficient based on the RH that the WetNeph provides, which changes over time.

PM10 gravimetric mass measurements

Unvalidated PM10 measurements from the measuring station Cabauw-Wielsekade are available during the TROLIX campaign. This data has been provided by Jan Vonk [RIVM]. The PM10 measurements contain the daily gravimetric mass measurements and can be compared to the mass measurements based on the chemical composition. Because this data is not yet validated, it is only used as reference material.

Table 4.3: Basic information on estimated aerosols species as measured or assumed during the CINDI campaign 2009

Aerosol species	Measurement technique and assumptions
SIA	Daily values of the mass concentration of sulfate (SO_4), ammonium (NH_4) and nitrate (NO_3) are measured by analysing daily loaded QMA filters.
OC / OM	The mass concentration of OC is measured by analysing daily loaded EC/OC filters. To calculate OM from OC, a factor of 1.8 is used. This factor is the ratio of total organic mass to organic carbon (OM/OC) based on the findings of Bergström et al. (2012)
EC	The concentration of EC is measured by analysing by daily loaded EC/OC filters. In addition, eBC is measured by the MAAF, which has a much higher temporal resolution but does not measure all EC. High temporal estimations of EC are estimated by applying a scale factor on the eBC measurement. This scale factor during the TROLIX campaign has a value of 1.20 which is the ratio between the total mean mass concentration of EC and eBC.
Sea Salt	Mass concentrations of Cl, Na, Mg, Ca and K are measured by analysing daily loaded Teflon and QMA filters.
Other	Some metals and minerals are taken into account because they could be measured by the Teflon daily filters. These are Al and Fe. The mass concentration of silicon can be calculated based on the Al/Si PM10 ratio of 0.29 which is based on average measurements in the Netherlands. Assuming that SiO_2 and Al_2O_3 are the most common minerals, the mass concentration of mineral dust can be calculated based on the measured mass concentration of Al.

4.3.2 Data processing

6 hour mean

All measured values during the campaign are converted to 6-hour mean values (00:00-06:00,06:00-12:00,12:00-18:00 and 18:00-00:00), so that every day has four measuring points, and thus diurnal patterns can be detected. All chemical mass concentrations, except for EC, are measured by analyzing daily filters, which means that the 6-hour-mean value is constant over the day. However, the PSD and WetNeph measurements are measured with high frequency which makes this 6h-mean approach possible.

Nephelometers

Prior to the start of the campaign and during the first days of the campaign (7-11 September), the working state of both nephelometers was tested to find possible biases between the two instruments. This five day period is called the 'testing period'. During this period both nephelometers have performed the same measurements, based on the same ambient air. The output can be seen in Figure 4.11 (RH) and Figure 4.12 (Scattering coefficient, only during the testing period). During this testing period, it was found that the two nephelometers measure different values of RH while analysing the same air and thus the same RH. Figure 4.11 shows this bias in measured RH during this testing period: The wet-setup (which contains the old nephelometer up to 11 September) measures lower RH values compared to the dry-setup (which contains the new nephelometer up to 11 September). So the old nephelometer measures lower RH-values. Due to the expected hotter conditions in the old nephelometer, the temperature of the air rises, lowering the RH within the instrument. This effect is more favorable for the dry setup as it will be easier for this nephelometer to reach RH values below 40%. Following this finding it was decided to switch the two nephelometers between the two setups. This way from September 11, the old nephelometer became part of the dry setup, measuring dry air. Due to the higher temperatures within this instrument, measuring low RH becomes easier. And vice versa, it is easier for the new nephelometer to enhance the RH of the air, so the new nephelometer will be used in the wet-setup to measure $\text{RH} \approx 85\%$. All measurements after 11 September have this setup.

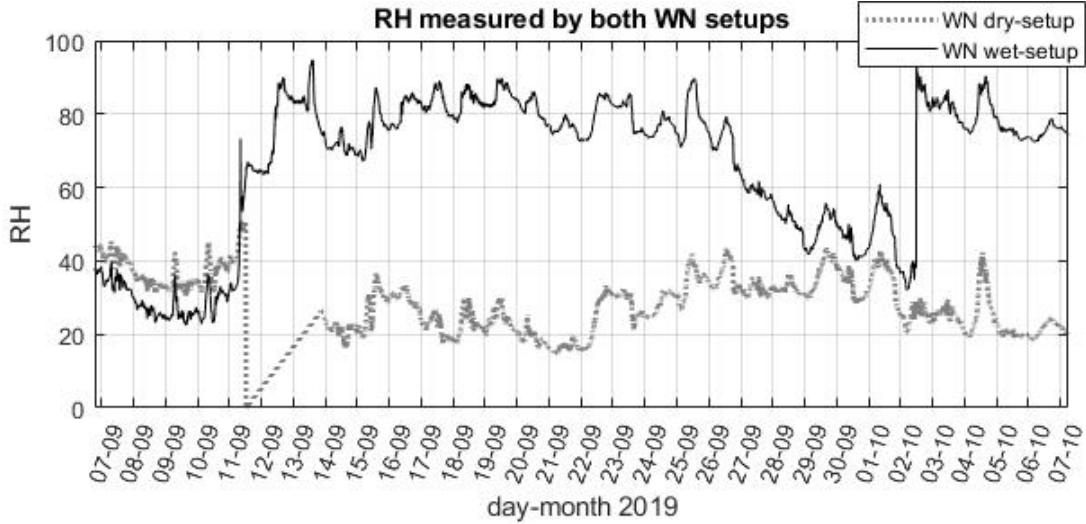


Figure 4.11: RH measured by both setups. Until 11 September, both setups measured the same air. After 11 September the air is dried or enhanced for the dry- and wet-setup respectively.

Figure 4.12 shows the scattering coefficient measured by both nephelometers during the testing period. Both instruments measure in dry conditions during this test period. (There are a few exceptions, but those are excluded to make sure the following calculations are based on dry conditions only). Under normal conditions the scattering coefficients of both nephelometers should be similar, within an error of about 5%, but a larger offset between both output values can be observed. This offset is probably caused by instrument differences and needs to be accounted for in order to calculate realistic enhancement factors at a later stage. The scattering coefficients have to be scaled so that they will become the same. This is done by using a scaling factor based on the output differences of the scattering coefficient. Figure 4.13 shows the output differences between the two nephelometer in the dry RH region ($RH < 40\%$). Assuming that the newest nephelometer measures most accurate it is decided to scale the outcome values σ_s of the old nephelometer to the new nephelometer by dividing it by a factor 1.21 (std=0.10), this is the mean factor between both coefficients $\sigma_{s,old} / \sigma_{s,new}$.

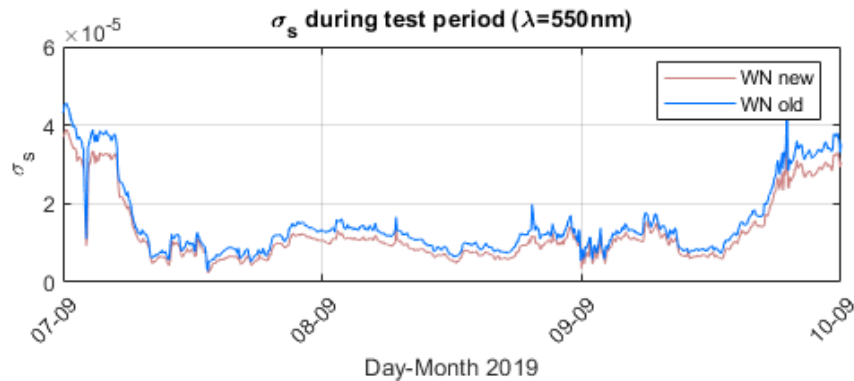


Figure 4.12: σ_s as measured by both nephelometer instruments during the test period only.

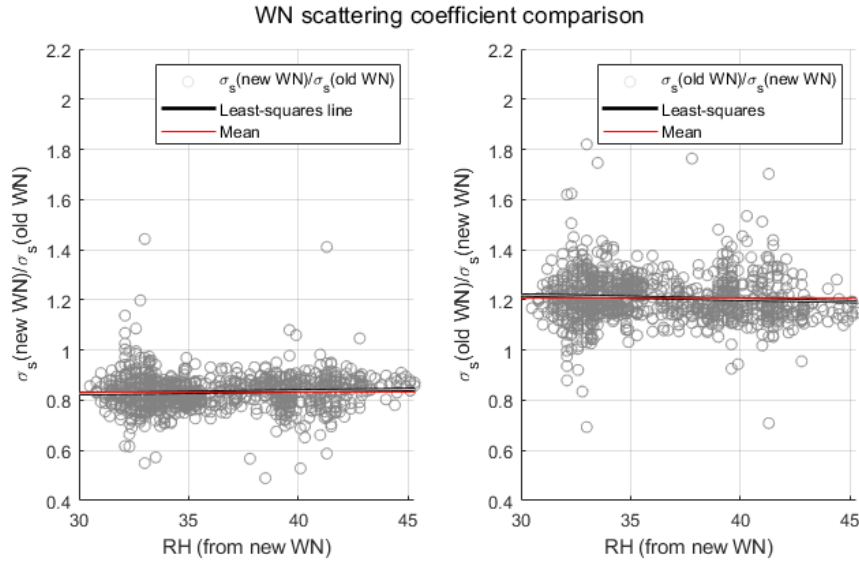


Figure 4.13: Comparison between the scattering coefficients of both nephelometer instruments (old and new) during parallel measuring in dry conditions (7-10 September 2019 for $\lambda = 550\text{nm}$). The trend which can be found is ignored as it is too small to have a significant effect.

Figure 4.14 shows the resulting scattering coefficients as measured by both nephelometers during the campaign days with a complete data set (14-23 September). The output of the dry nephelometer is adjusted according to the scale factor to compensate for the deviation discussed above. With the new output, the enhancement factor can be calculated using Equation 2.5. It should be noted here that the enhanced RH is not fixed to one value but has a range between 70-90%, this is visualized in the bottom graph of Figure 4.14. These values are later compared to the H-model output values.

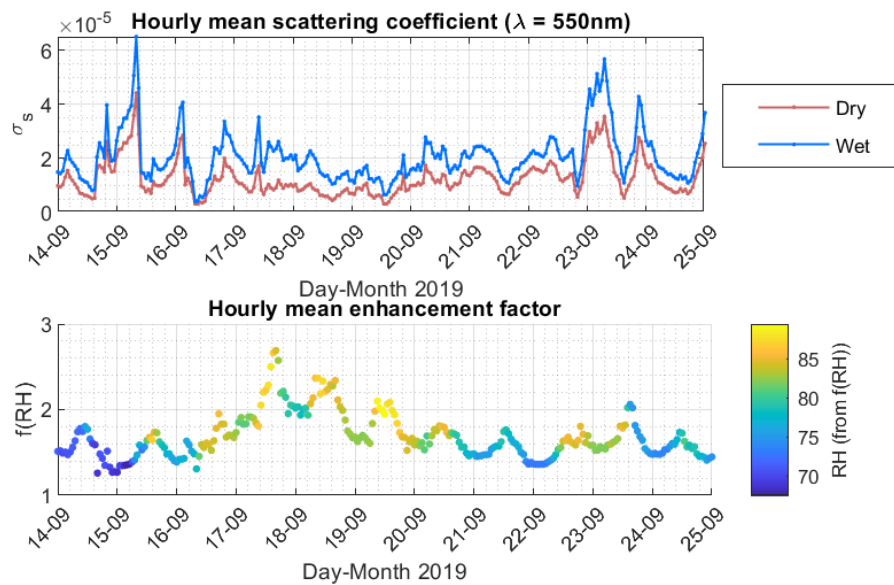


Figure 4.14: Hourly mean scattering coefficient measured in dry conditions and with enhanced RH ($\lambda = 550\text{nm}$) [Top]. Including the scattering enhancement factor for each specific measurement moment [Bottom].

H-model

The H-model calculates the scattering and enhancement factors based on the 6-hour mean values of the in situ measurements.

The results from the CINDI campaign data suggested that the growth factor calculated by ISORROPIA might be too large. To make sure that the ISORROPIA growth factor is realistic, it is compared to the growth factor calculated by κ -Köhler theory (called the 'Kappa approach') (Petters and Kreidenweis, 2007). The diameter growth factor, according to the κ -Köhler theory can be approximated as follows (Petters and Kreidenweis, 2007):

$$g_D(RH) = \left(1 + \kappa \frac{RH}{1 - RH}\right)^{1/3} \quad (4.1)$$

In the H-model the enhanced RH as measured by the WetNeph will be used as input. Notice that this value changes for all measuring moments. κ is a value which describes the hygroscopicity of the aerosol assemble and can be calculated with a mixing rule:

$$\kappa = \sum \epsilon_i \cdot \kappa_i \quad (4.2)$$

where κ_i is the κ -value per specific aerosol species (see Table 4.4) and ϵ_i is the volume fraction of each specific aerosol species.

The κ -Köhler theory estimates a growth factor which is expected to be close to the true value of the real growth factor of the aerosol mixture. However, the growth factor calculated using κ values is also just an approximation of the true value. Not only are the kappa values an average value for the species they represent, these values may also differ as a function of particle size and solute concentration, which is ignored in the approach used in Equation 4.1 and 4.2 (Wang et al., 2017). Both approaches will calculate a growth factor which will be compared to each other to judge whether both values are similar and to identify erroneous answers. In addition, the H-model is run twice: Once with the growth factor based on ISORROPIA and once based on κ -Köhler theory.

Table 4.4: Hygroscopic coefficient κ per aerosol species (Petters and Kreidenweis, 2007)

Aerosol species	κ
Black carbon	0.0
Organics	0.1
Sea salt	1.0
Sulfate	0.5
Ammonium	0.7
Nitrate	0.7
Dust / other	0.0

Extra model runs

From the results of the TROLIX model runs (which are not yet discussed) it becomes clear that the enhancement factors calculated by the H-Model are larger then those measured by the nephelometers. Besides other potential errors that have already been mentioned, another possible explanation of this behaviour could be an underestimation of the temperature in the sensing volume of the Nephelometers and thus an overestimation of the RH. It is known that at the sensing volume the temperature is much higher due to the measuring technique of the nephelometer, causing the local RH to drop. This is also why in the new nephelometer a heat shield is added to partially counteract this effect. The nephelometer measures the internal RH and temperature, however these values may differ from the RH and temperature at the sensing volume, because the internal values are measured just after the sensing volume and not directly at the sensing volume. As a result, the reading of the RH is expected to be too

high so the RH in the sensing volume of the nephelometers might be lower. This is no problem for the dry nephelometer, because this would mean that the measurements will be even drier than before. However, the scattering coefficients of the wet nephelometer are used to calculate the enhancement factor based on the given RH of the nephelometer. A wrong RH results in calculations that won't match the measurements. A decrease in the measured RH can be calculated so that the calculated and measured enhancement factor will match (best). To find out what change in RH would result in the best overlapping enhancement values, it was decided to include multiple H-model runs with lower RH values.

A percentage reduction is applied on the RH measured by the WetNeph. The entire H-model run (with κ -Köhler theory) is repeated for different lower values of RH.

$$RH_{i,\#run,reduced} = RH_i \cdot (1 - 0.01 \cdot \#run) \quad (4.3)$$

where i is every measuring moment and $\#run$ is a value between 0 and 100. In every run, all measured RH values are reduced by 1% to measure the effect on the calculated enhancement factors. For every run, the mean difference between the $f(RH)_{WetNeph}$ and $f(RH)_{H-model}$ can be calculated until the best match is found for a given RH reduction. For every $\#Run$, the mean difference between the calculated and measured enhancement factors of all measuring moments is calculated. The run with the lowest mean difference is assumed to be the best match. To find the temperature difference that could cause such a RH difference the August-Roche-Magnus approximation is used to calculate corresponding temperatures (Alduchov and Eskridge, 1996).

4.3.3 Results from the TROLIX campaign

All results are 6h-mean values from 14 to 22 September. In order to see diurnal fluctuations, the results are visualized in chronological order.

Mass and volume concentrations

Figure 4.15 visualizes the aerosol mass and volume concentration based on the measurements of the PSD and chemical composition. The daily mass concentrations based on the measurements of the chemical composition are always below the value of the PM10 gravimetric mass measurements. The chemical mass concentration accounts for 63-98% of the total aerosol mass on different days of the campaign, so not all aerosols are captured with the filter measurements. In the same figure, the PSD is converted to an estimated mass concentration by assuming a specific average density. Regardless of the chosen mean aerosol density, it can be seen that the PSD clearly shows fluctuations during the day, which is expected to be caused by daily fluctuations of secondary aerosols. The daily filters and PM10 measurements do not capture these fluctuations as they are daily mean values (with the exception of the EC measurements). But it can be concluded that the daily fluctuation of the mass concentrations can be quite large according to the PSD measurements as daily values can differ up to $10 \mu\text{g}/\text{m}^3$.

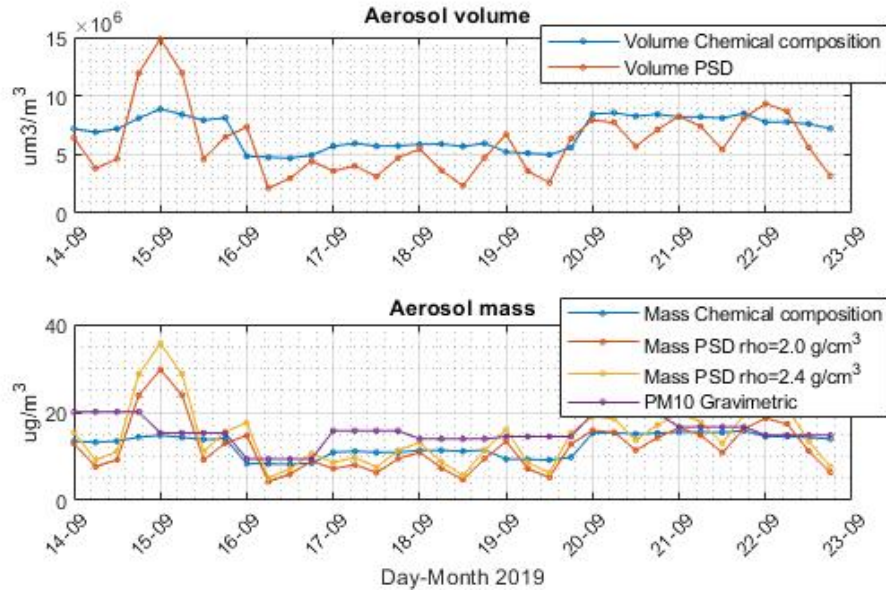


Figure 4.15: Mass and volume comparison of different measurement techniques during the entire campaign period

Diameter growth factor

The diameter growth factor is calculated with both the ISORROPIA and the κ -Köhler theory as can be seen in Figure 4.16. Both calculations result in a growth factor with a similar order of magnitude and fluctuation. The correlation between both factors is strong ($r=0.85$). The relative difference between growth factor (κ -Köhler/ISORROPIA) has a maximum of $\pm 13\%$. Because the results from ISORROPIA correlate with those from κ -Köhler theory, it is decided to investigate the effects of both diameter growth factors on the scattering coefficients calculated by the H-model.

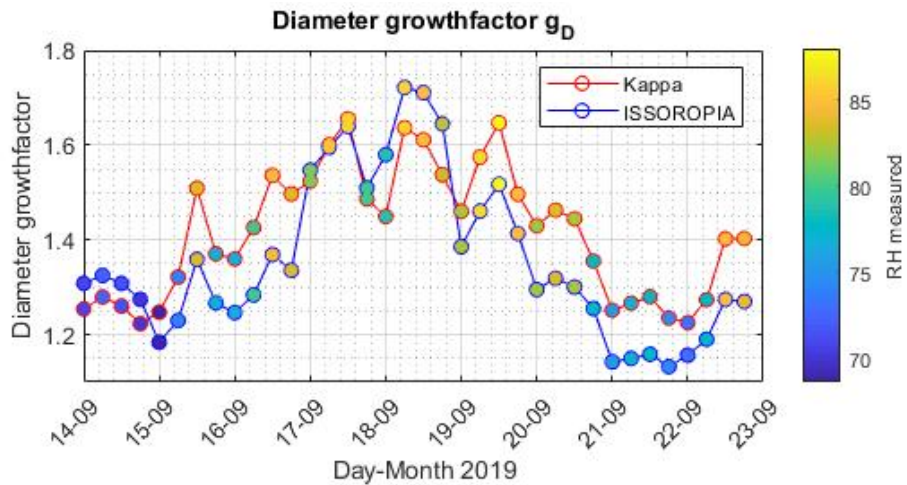


Figure 4.16: Diameter growth factor (using ISORROPIA and κ -Köhler theory), including the enhanced RH on which the growth factors are based.

Scattering and enhancement factors

Figure 4.17 shows the calculated and measured scattering coefficients for dry and enhanced conditions and the resulting enhancement factors. The black line shows the values as measured by the nephelometers. The blue and red lines show the results of the H-model using growth factor values calculated by ISORROPIA and κ -Köhler theory, respectively. Notice that the calculated dry scattering coefficient is the same for the Kappa and ISORROPIA approach.

There seems to be a difference between the scattering coefficients calculated by the H-model and measured by the nephelometers. By comparing the dry scattering coefficients (the dashed lines in Figure 4.17), it can be seen that the correlation is strong ($r=0.89$) but the calculated value is a factor 1.8 (std=0.34) larger compared to the measured value. This difference in scattering coefficients confirms that the calculations of the scattering coefficients do not yet match the measured coefficients, but this difference will not affect the enhancement factor as this is a function relative to the dry scattering coefficient. This is why the scattering enhancement results can be addressed separately.

The calculated and measured enhancement factors show similar fluctuations (Top Figure 4.17). The H-model run with ISORROPIA correlates slightly better with the measured value compared to the Kappa approach ($R=0.84$ and $R=0.76$ respectively). But as can be seen as well in the Figure 4.17 (top), the results calculated by the H-model overestimate the true enhancement factors (if the WetNeph is assumed to be correct). Figure 4.18 and 4.19 show the correlation between the H-model and the WetNeph enhancement factor for the ISORROPIA and κ -Köhler approach respectively. Because the difference in the enhancement factors seems to be RH dependent, an additional scatter plot is created to visualize whether this is indeed the case (Figure 4.20 and 4.21). The difference between the calculated and measured enhancement factors seems to increase with RH. This trend is not completely unexpected because the enhancement factor is more sensitive to small errors at high RH values than at low RH values.

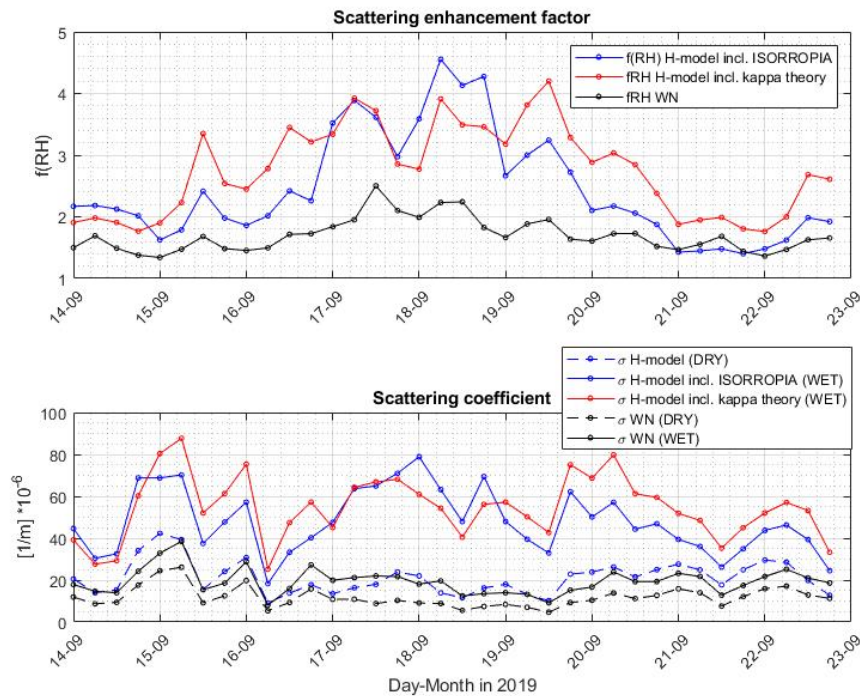


Figure 4.17: Enhancement factors and scattering coefficients as measured by the WetNeph and calculated by the H-model (using ISORROPIA and κ -Köhler theory for $\lambda = 550\text{nm}$).

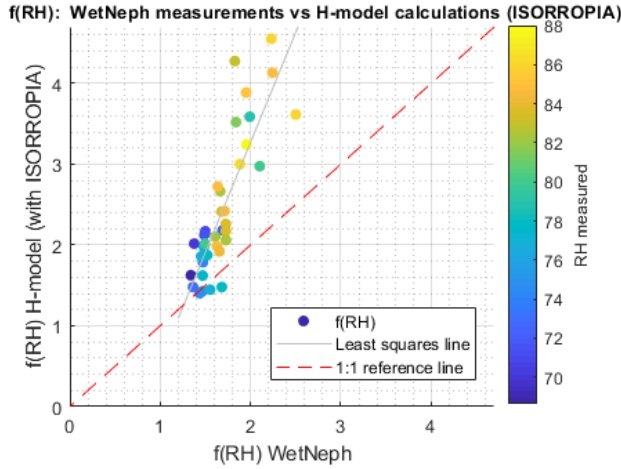


Figure 4.18: Comparison of the $f(RH)$ results. (The H-model includes ISORROPIA.)

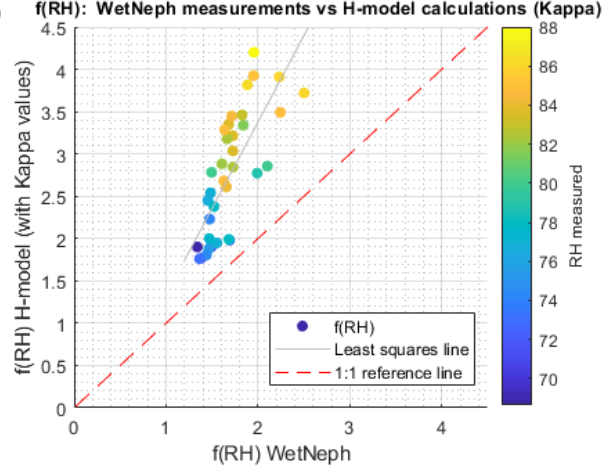


Figure 4.19: Comparison of the $f(RH)$ results. (The H-model includes the Kappa approach.)

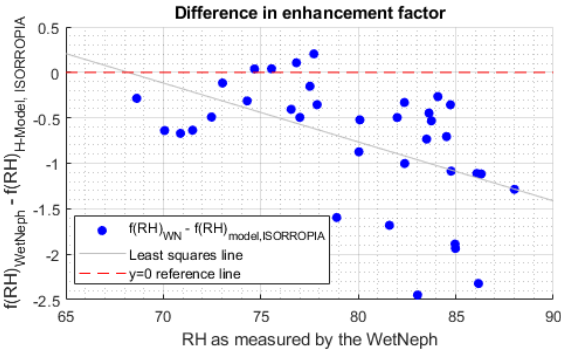


Figure 4.20: The difference between $f(RH)$ calculated and $f(RH)$ measured as a function of RH. (The H-model includes ISORROPIA.)

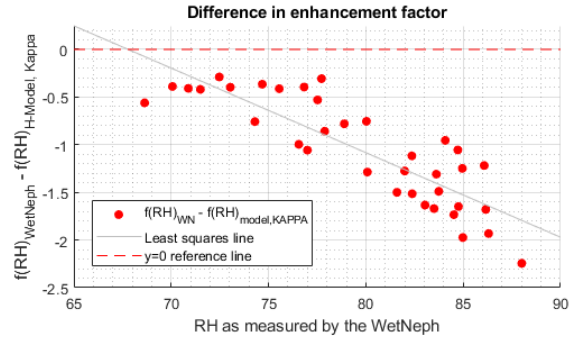


Figure 4.21: The difference between $f(RH)$ calculated and $f(RH)$ measured as a function of RH. (The H-model includes the Kappa approach.)

Closer look into the (large) enhancement factors of the H-model

The calculated enhancement factors are larger than the measured factors for the majority of the measurements (Top Figure 4.17). To understand what causes these large enhancements, we will have a closer look at the enhancement factor itself. The scattering enhancement depends on the enhancement of the total aerosol cross section ($G_{enhancement}$) and the change of the total scattering efficiency ($Q_{enhancement}$) (Equation 2.6). For every calculation the cross section enhancement can be easily calculated as it is the squared value of the growth factor:

$$G_{enhancement} = g_D(RH)^2 \quad (4.4)$$

The assumed efficiency enhancement can then be calculated using Equation 2.6 as it is the remaining variable. The $G_{enhancement}$ and $Q_{enhancement}$ can also be calculated by directly using the output variables of the H-model (G_{dry} , G_{wet} , Q_{dry} and Q_{wet}) which result in the same values.

Figure 4.22 shows the division of the calculated enhancement factor into $G_{enhancement}$ and $Q_{enhancement}$. The quantity of the cross section enhancement is acceptable as the κ -Köhler theory gives a good approximation of the diameter growth factor and ISORROPIA does not differ a lot from that. Note that the efficiency enhancement, which represents all particles of the PSD, is always larger than unity. This means that the MIE-model calculates an enhancement in total aerosol efficiency. Figure 4.23 shows the aerosol scattering efficiency curve for single wet and dry aerosol particles. This graph is created as an example and is based on the chemical composition measurements

on 23-09-2019 00:00-06:00. A scattering efficiency enhancement of larger than 1 means that all particles within the PSD together create a larger scattering efficiency for wet particles than for dry particles. Within the PSD, some particles become more (scattering) efficient and some become less (scattering) efficient, but all added together, the PSD becomes more effective. The dry and wet particle size distributions, as measured on 23-09-2019 00:00-06:00, are positioned in such a way that the wet particle size distribution in combination with the wet scattering efficiency curve of Figure 4.23 has an overall larger scattering efficiency compared to the dry particle size distribution. A more in depth explanation and example of the coherence of the PSD and the scattering efficiency curve will be discussed later with the help of Figure 4.30.

If it is assumed that the measured nephelometer enhancement values are the true values, an explanation has to be found as why the calculated values are too high. In order to decrease the calculated enhancement factor, so that it matches the measured value of the nephelometers, it can be concluded that either the cross section enhancement or the efficiency enhancement is too high and needs to decrease (or both). The cross section growth based on κ -Köhler theory is an often used approach in the literature that has a relatively small uncertainty. As result, its likely that the largest error component can be found in the calculated efficiency factor if a smaller enhancement factor is to be expected. To create a smaller scattering efficiency, the particle distribution within the PSD needs to change (see, for example, the results in Figure 4.27 which will be discussed later). This might suggest that the PSD based on the SMPS and APS during this campaign is not entirely correct.

Another possible explanation for the large calculated enhancement factor is that the RH is measured with an error by the WetNeph. The cross section growth factor and the efficiency growth factor both decrease with a smaller RH. This possible event is tested and is discussed later with the help of Figure 4.24.

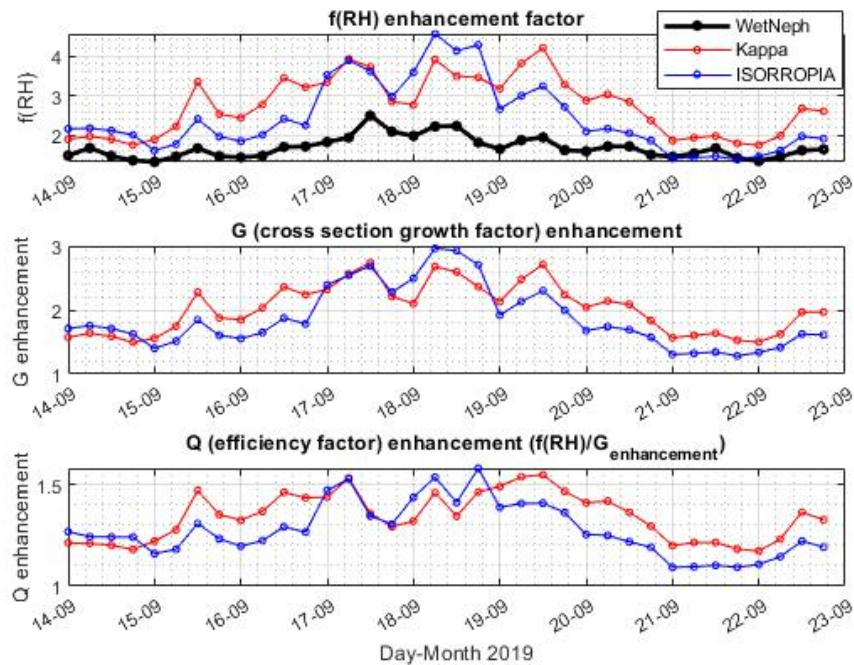


Figure 4.22: The enhancement factor split up into cross section enhancement and scattering efficiency enhancement (using $\lambda = 550\text{nm}$).

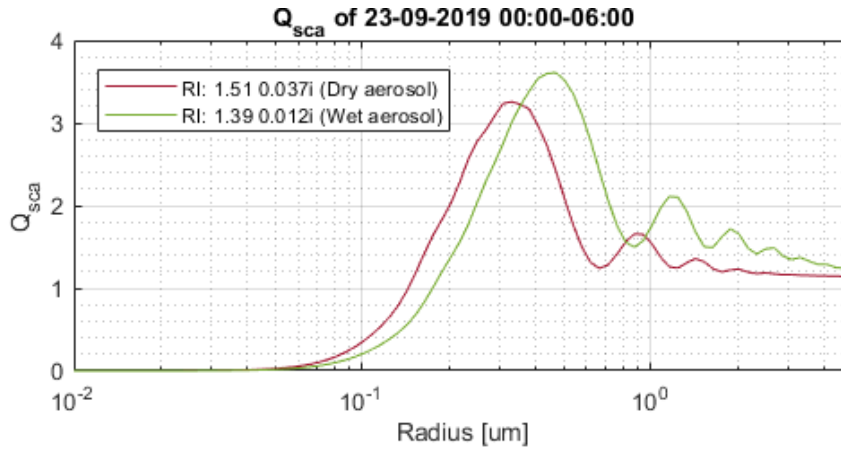


Figure 4.23: Example of the aerosol scattering efficiency of a single aerosol particle (dry or wet) as a function of its radius (for $\lambda = 550\text{nm}$). The graph is a smoothed visualization.

Nephelometer assumptions

Assuming that the WetNeph might overestimate the RH at the sensing volume, the H-model (with κ -Köhler theory) was run several times with a decreased RH to find the value that will result in an enhancement factor of the H-model that best fits the WetNeph results. A 20% decrease in RH results in the best fit, the effect of this reduction on the scattering enhancement can be seen in Figure 4.24. If it would be assumed that the RH at the sensing volume of the WetNeph is indeed 20% lower, this would mean that the temperatures at the sensing volume are approximately 4 degrees higher than the ones measured in the WetNeph. However, due to the relative fast aerosol flow through the nephelometer, the aerosol mixture is expected to be in a transient equilibrium. To reach 20% lower RH, the temperature difference probably should have been a little more than 4 degrees.

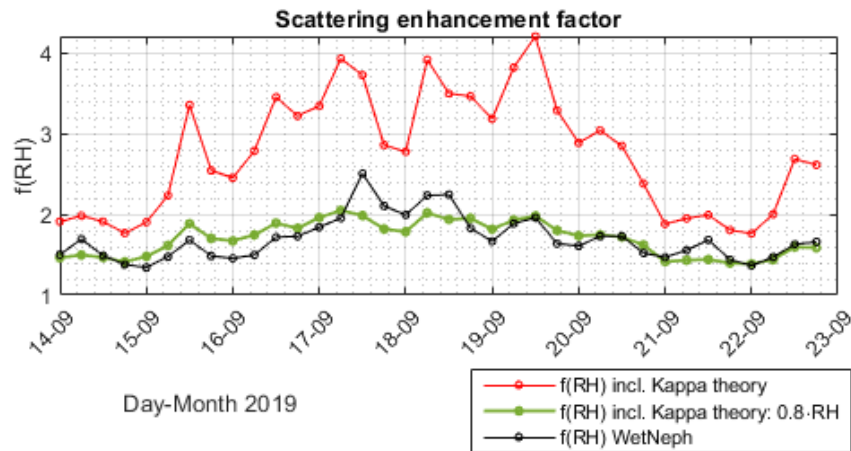


Figure 4.24: Measured scattering enhancement(WetNeph) versus calculated scattering enhancements (κ -Köhler) based on the RH measured by the WN and 0.8 times the RH ($\lambda = 550\text{nm}$).

A 20% decrease of the RH, results in lower calculated enhancement factors that match better with the measured enhancement factors. As a result, the difference between the measured and calculated enhancement factors decreases, as shown in Figure 4.25. In addition, the RH dependence of the difference between the calculated and measured enhancement factor is negligible for this calculation (Figure 4.26). This in contrast to the original calculations which seem to be strongly RH dependent. It has to be mentioned however, that the RH values of the calculation with the decreased RH in Figure 4.26 are of course lower than the original calculations. The trend at lower RH is expected to be weaker as well, due to the lower hygroscopic behaviour of the aerosols in this region.

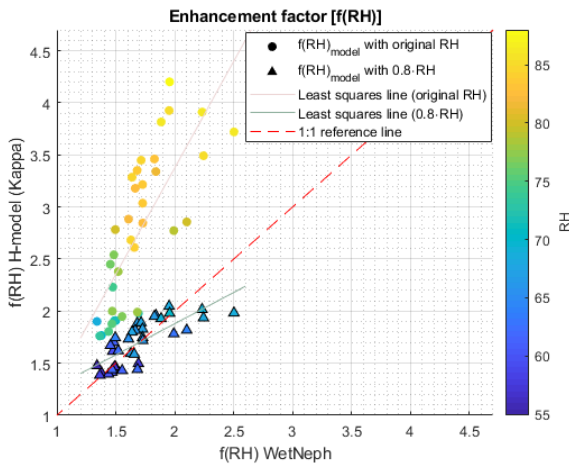


Figure 4.25: Comparison between measured (by the WetNeph) and calculated (by the H-model) enhancement factors. The H-model uses the original RH values (as measured by the WetNeph) and decreased RH ($0.80 \cdot RH$). (The H-model includes the Kappa approach.)

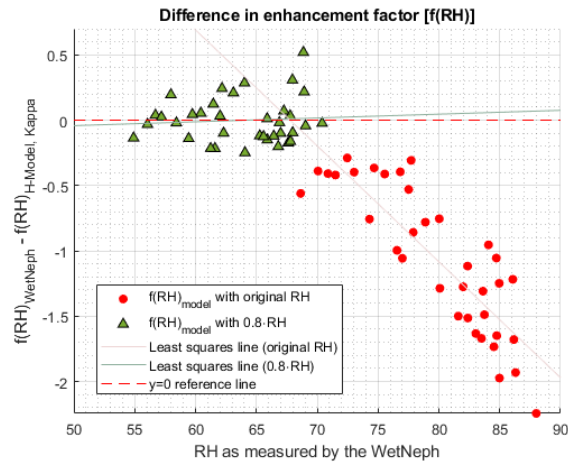


Figure 4.26: The difference between $f(RH)$ calculated and $f(RH)$ measured as a function of RH. The model uses the original RH values (as measured by the WetNeph) and decreased RH ($0.80 \cdot RH$). (The H-model includes the Kappa approach.)

The effect of small and large aerosol particles

The enhancement calculation is run twice more. The first extra run uses the original merged particle size distribution, but without all particles with a diameter below $0.04\mu\text{m}$. In this study it was assumed that small particle sizes do not significantly affect the scattering coefficients and thus the scattering enhancement of the aerosol mixture. This is why the small ranges of the SMPS ($D < 0.04\mu\text{m}$) could easily be adjusted in subsection 4.3.2. Figure 4.27 shows the enhancement factor of the original PSD (red line) and the enhancement factor based on the PSD without these small particles (dashed cyan line). These results confirm that the enhancement factor is not affected if small particle sizes are completely ignored, because the calculations of the scattering enhancement factors are the same for a PSD with and without small particles. This can be explained by looking at the efficiency curve of Figure 4.23 which shows negligible values for particles having a radius below $0.05\mu\text{m}$.

The second extra run is based on the original PSD, but with an increased amount of aerosol particles having diameters larger than $0.6\mu\text{m}$. This new PSD is created by merging the APS to the SMPS with an effective density of 2.0 instead of 2.4 g/cm^3 , which results in more larger particles (see Figure 4.10 for a mean example). In this study it was decided to merge PSD of the APS and SMPS by assuming a effective density of 2.4 g/cm^3 as this high density value creates a smooth transition between the two particle size distribution. But by doing so, the number concentration for bigger particles may have been underestimated. The effect of this adjustment on the enhancement factor can be seen in Figure 4.27: The red line shows the enhancement factor of the original PSD, which is based on an effective density of 2.4 g/cm^3 . The solid cyan line shows the enhancement factor based on the PSD with more larger particles, which is based on an effective density of 2.0 g/cm^3 . The scattering enhancement factor of the PSD with more larger particles is slightly lower compared to the enhancement factor of the original PSD for most data points.

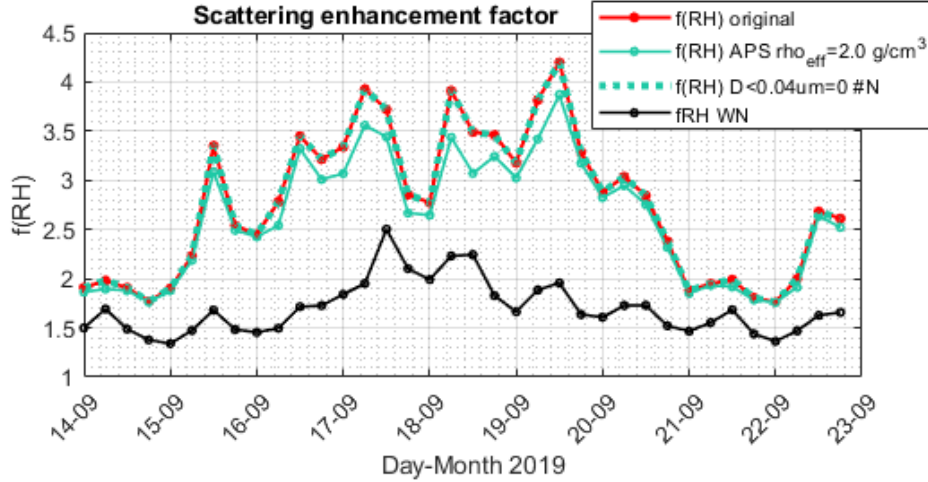


Figure 4.27: Aerosol scattering enhancement ($\lambda = 550\text{nm}$). The figure shows $f(\text{RH})$ as measured by the WetNeph (black line) and the original calculation by the H-model (red line). In addition the H-model calculated the $f(\text{RH})$ for a PSD with no small aerosol particles (dashed cyan line) and the $f(\text{RH})$ for a PSD which includes more larger particles (solid cyan line).

Adding more larger particles, in this case, leads to lower calculated enhancement factors. Figures 4.28 and 4.29 visualize the effect of adding larger particles to the PSD on the enhancement difference between the measured and calculated enhancement factor. Figure 4.29 shows that the decrease in enhancement factor is the largest for measurements with a high RH. Therefore, it can be concluded that assuming a higher count of larger particles has the most effect on calculations at high RH.

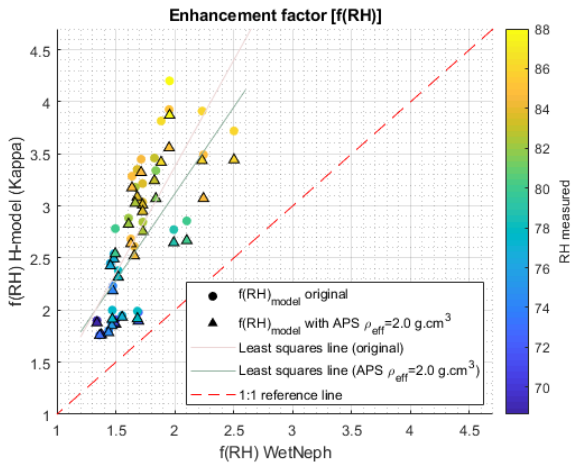


Figure 4.28: Comparison between measured (by the WetNeph) and calculated (by the H-model) enhancement factors. The H-model uses the original PSD ($\text{APS } \rho_{\text{eff}}=2.4$) and PSD with an increased amount of large particles ($\text{APS } \rho_{\text{eff}}=2.0$). (The H-model includes the Kappa approach)

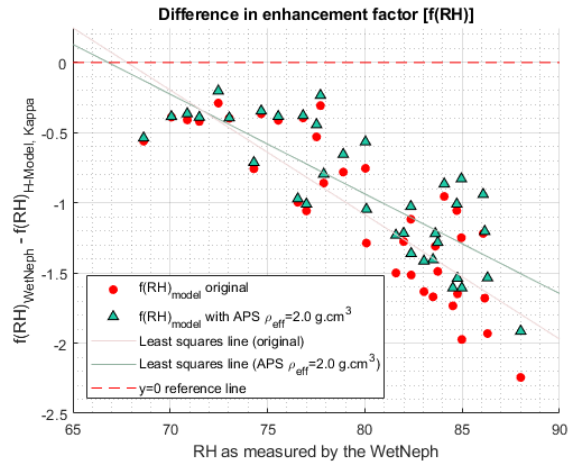


Figure 4.29: The difference between $f(\text{RH})$ calculated and $f(\text{RH})$ measured as a function of RH. The H-model uses the original PSD ($\text{APS } \rho_{\text{eff}}=2.4$) and PSD with an increased amount of large particles ($\text{APS } \rho_{\text{eff}}=2.0$). (The H-model includes the Kappa approach)

A decrease in the enhancement factor due to including more larger aerosol particles in the PSD is not really straightforward. An example will be discussed below to create a better understanding of the scattering enhancement factor and the role that the scattering efficiency (Q_{scat}), the cross section (G) and scattering coefficient σ_{scat} play in this. For this, a comparison will be made between an 'original PSD' and a 'large PSD' which have the same chemical composition, but only a slightly different PSD. The large PSD has a larger amount of aerosol particles with diameters larger than $0.6\mu m$, the same as discussed above.

Tables 4.5 and 4.6 show an example of the calculated scattering properties of the 'original PSD' and the 'large PSD' in which the scattering enhancement of the 'large PSD' is smaller compared to the 'original PSD'. Dry and wet conditions are described, so that the enhancement factors can be explained. The following differences are important:

- The total cross section (G_{total}) describes the cross section of all aerosols particles of the PSD combined. It therefore makes sense that the 'large PSD' has a larger G_{total} in dry and wet conditions compared to the 'original PSD', due to the extra aerosols in the 'large PSD'. But, the cross section enhancement (the growth of the particles) is similar for both PSDs, because this is based on the chemical composition of the PSD which is the same for both PSDs.
- The total scattering efficiency ($Q_{scat,total}$) is the scattering efficiency that represents the entire PSD. The 'large PSD' has a larger $Q_{scat,total}$ in dry and wet conditions compared to 'original PSD', but the scattering efficiency enhancement is smaller for the 'large PSD'.
- The total scattering coefficient ($\sigma_{scat,total}$) in dry and in wet conditions is higher for the 'large PSD' due to a larger total cross section and a larger total scattering efficiency. But the scattering enhancement, on the other hand, is smaller for the 'large PSD' due to the lower scattering efficiency enhancement.

Table 4.5: Scattering properties of the 'original' PSD (as shown in Figure 4.30)

Original PSD		Dry	Wet	Enhancement
Total cross section	G_{total}	$1.71 \cdot 10^1 [\mu m^2 / cm^3]$	$4.50 \cdot 10^1 [\mu m^2 / cm^3]$	2.63 [-]
Total scattering efficiency	$Q_{scat,total}$	$6.79 \cdot 10^{-1} [-]$	$9.00 \cdot 10^{-1} [-]$	1.33 [-]
Total scattering coefficient	$\sigma_{scat,total}$	$1.16 \cdot 10^1 [Mm^{-1}]$	$4.05 \cdot 10^1 [Mm^{-1}]$	3.49 [-]

Table 4.6: Scattering properties of the 'large' PSD (as shown in Figure 4.30)

Large PSD		Dry	Wet	Enhancement
Total cross section	G	$1.87 \cdot 10^1 [\mu m^2 / cm^3]$	$4.92 \cdot 10^1 [\mu m^2 / cm^3]$	2.63 [-]
Total scattering efficiency	$Q_{scat,total}$	$8.75 \cdot 10^{-1} [-]$	1.07 [-]	1.22 [-]
Total scattering coefficient	$\sigma_{scat,total}$	$1.64 \cdot 10^1 [Mm^{-1}]$	$5.26 \cdot 10^1 [Mm^{-1}]$	3.23 [-]

Although the scattering coefficient of the 'large PSD' has larger values for both dry and wet conditions when compared to the 'original PSD', this does not mean that the enhancement factor is larger as well. We have seen that the cross section enhancement is similar for both PSDs, so the lower scattering enhancement of the 'large' PSD can only be explained by the lower scattering efficiency enhancement. The original and large PSD both grow in total efficiency when they absorb water (from dry to wet particles), but the original PSD grows much more in efficiency compared to the large PSD.

To understand this difference in enhancement a little better, Figure 4.30 shows the different scattering properties per bin. Figure 4.30a shows the original and large PSD for dry and enhanced conditions. In addition, it shows a simplified scattering efficiency line (Q_{scat}) for dry and wet particles. This line shows the scattering efficiency of a single particle as a function of its radius. For dry particles, particles with a radius between 0.2 and $0.5 \mu m$ are the most efficient. If the particles are wet, the efficiency curve shifts towards larger particle sizes, then particles with a radius between 0.3 and $0.7 \mu m$ are the most efficient. By comparing the 'original' and 'large' PSD, it can be clearly

seen that the large PSD has more aerosol particles in the most effective region of the scattering efficiency curve. This applies to both the dry and wet PSD relative to the dry and wet Q_{scat} .

When calculating the scattering coefficient, the combined cross section of all particles is more important than the number of particles. So, in Figure 4.30b the total cross section per bin (G_{bin}) is compared to the Q_{scat} .

$$G_{bin} = (\pi \cdot r_i^2) \cdot N_i \quad (4.5)$$

where r_i is the radius of the particle of the selected bin and N_i is the total number of aerosol in this bin. The difference between the 'original' and 'large' PSD becomes more clear as larger particles have a larger cross section.

The scattering coefficient per bin can be calculated by multiplying the G_{bin} with Q_{scat} . Figure 4.30c then shows the scattering coefficient per bin. If you add the scattering coefficients per bin for a specific PSD, this results in the total scattering coefficient as mentioned in Table 4.5 and 4.6. Figure 4.30c shows that for this PSD the particles in between $r=0.1$ and $1\mu m$ contribute the most to the final calculation of the scattering coefficient (note the logarithmic distribution of the y-axis). For the dry PSD this range is a little lower compared to the wet PSD. Due to the total cross section and scattering efficiency per bin, the PSD is very sensitive to changes in this regime. It also causes that the enhancement factor in the end is lower for this larger PSD.

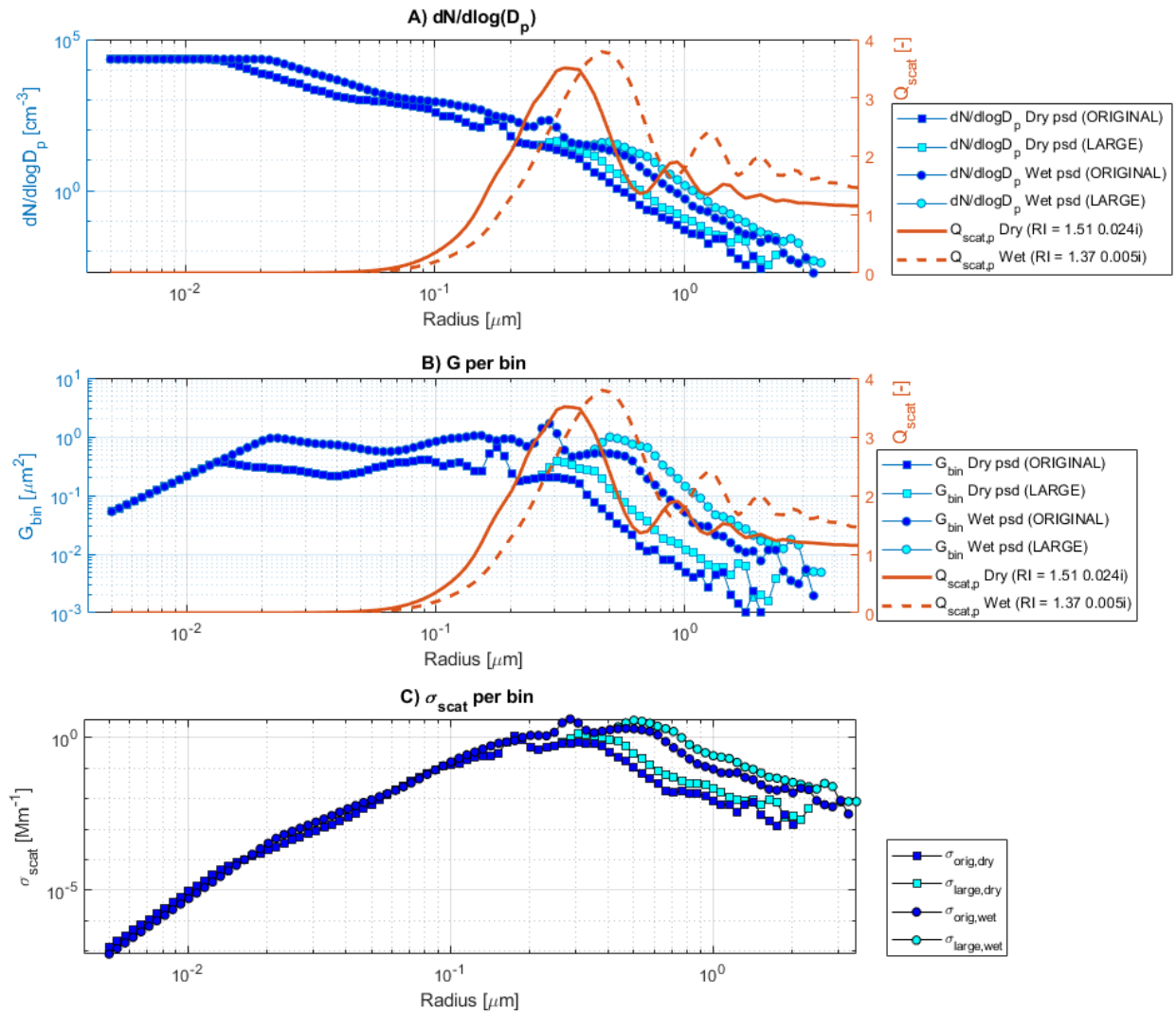


Figure 4.30: Example of the bin-wise calculation of the scattering coefficient based on the scattering efficiency (Q_{scat} and cross section G). Sub-figure A shows the original and wet PSD in dry and wet conditions in combination with the dry and wet scattering efficiency curve. Sub-figure B shows the total cross section per bin for all PSDs in combination with the dry and wet scattering efficiency curve. Sub-figure C shows the scattering coefficient per bin for all PSDs.

5 Discussion and conclusion

5.1 Discussion

In this study, the H-model is created in order to estimate atmospheric scattering properties based on dried aerosol in situ observations such as chemical composition and particle size distributions. This model is tested by comparing the calculated scattering properties with those measured by WetNeph measurements. Although the measured and calculated results do not yet match perfectly, a strong correlation is observed between both data sets. This shows that the H-model is able to process changes in PSD or chemical composition into the enhancement factors. The differences between calculated and measured results cannot be explained entirely by the known uncertainties. As can be seen in the validation results, there are multiple suggestions to improve the results or explain part of the differences. These suggestions are not just about improving the H-model, but also about checking on the input variables and the WetNeph measurements themselves. In general, the H-model, the input values and WetNeph measurements all influence the agreement between the calculated and measured scattering values. The H-model itself is not yet optimized and can be improved. In addition, input values, on which the calculations are based, do influence the results as well. The accuracy and precision of the input variables are rather important as small changes have a significant effect on the calculated results. Last but not least, the measurements performed by the WetNeph might deviate from the ground truth. Shortly, all three options will be discussed below based on the findings of this report.

5.1.1 Discussion on the H-model

The hygroscopic behaviour of the aerosols is estimated with the ISORROPIA model. When calculations from ISORROPIA are compared to the κ -Köhler theory predictions, it can be concluded that both approaches find similar dependencies on chemical composition. The κ -Köhler theory includes the (small) hygroscopic growth of organic aerosols which ISORROPIA ignores, because ISORROPIA only takes SS and SIA particles into account. The ISORROPIA model, on the other hand, includes the expected aerosol combinations (solid, liquid and gaseous) resulting from the chemical input data, the temperature and RH. The future possibilities for a model such as ISORROPIA seem more promising as it can distinguish multiple aerosol combinations. This can also be seen in the results from the sensitivity study of ISORROPIA. Removing or reducing certain aerosol species from the aerosol mixture results in significant changes of the growth factor. This is something that is not included in the κ -Köhler approach as it does not distinguish between different elements within the species groups. ISORROPIA is certainly a good addition to the H-model. Especially at high temporal measurement resolution, it might even be a better approach than the κ -Köhler approach as it can notice small variables within the chemical composition and incorporate this into a changing growth factor. However, while the possibilities of ISORROPIA seem promising, it is important that all different elements within the model are better understood in order to work optimally.

The MIE-theory is used to calculate the scattering coefficient based on the measured PSD and RI. Instead of using a standard lognormal aerosol distribution, the MIE-sizedis model calculates the scattering properties based on a PSD that is divided in 100 bins. This approximation calculates the scattering coefficient within a 2% error margin and cannot be responsible for the offset between measured and calculated scattering properties that is found during the campaign.

The H-model uses a volume-weighted RI and mean density values for different aerosol species. The effective RI of the entire aerosol mixture is calculated by using the volume fraction of each aerosol species based on its density. Also the remaining aerosol particles that do not belong to one of the main aerosol groups have an estimated mean value for density but are not included in the calculation of the RI. However in this model, only the SIA, OM, EC, SS and water fractions are used. The 'other' part of the aerosols, which contains remaining metals and minerals, is not defined. It might be good to investigate the difference it would make if those aerosols were to be included into the estimation of the RI of the aerosol mixture. For this, a mean value of the RI has to be assumed for these remaining

metals and minerals. Although the volume fraction of these remaining particles is generally low, the associated small differences might have a small measurable impact on the outcome.

The H-model allows its user to create a simplistic representation of the real ambient conditions of the aerosols. The current model assumes that the chemical composition within a PSD remains constant over and is independent of the aerosol radius. Therefore, it is assumed that all particles grow with the same growth factor. To improve the model it would be good to adapt it so that it accepts a chemical composition input which is size-dependent. Especially because it was shown that large aerosol particles do have a direct effect on the enhancement in contrast to small particles and in general large particles will grow more, partly due to the higher concentration of hygroscopic aerosols. A first step would be to distinguish between PM_{2.5} and PM₁₀. Another approach would be to use common distributions of specific aerosols such as EC, SS or SIA. An estimation of the percentage-wise distribution of the chemical composition within each size bin can then be made. By doing so, each size bin will have a different RI, hygroscopicity and growth factor. This will result in a more realistic outcome of the calculated scattering and enhancement values.

5.1.2 Discussion on the input values

To improve the quality of the results from the H-model and to decrease the difference between calculated and measured results, it is also important to look at the observational errors of the input data.

The chemical composition is measured by combining the mass concentration of different aerosol elements. The daily mean outcome is realistic as the mass concentration based on the chemical composition approaches the same concentration as measured by the PM₁₀ gravimetric measurements for most days. So, overall the measurements on aerosol chemical composition seemed correct. But, on a few days up to 37% of the mass concentration was not captured by filter measurements which is likely to have caused an error in the calculation of the diameter growth factor and refractive index. In addition, the data on chemical composition could be improved by using a higher temporal resolution. Especially secondary aerosols fluctuate during the day due to e.g. temperature variations. This could also partly explain the difference in aerosol volume measured by the PSD and measured by the mass concentration measurements as seen in Figure 4.15. An option to do so is to use the MARGA instrument to measure secondary inorganic aerosols. During the TROLIX campaign, the MARGA was running. The data set of this study could be improved by combining this information once the data is released, so that the effect of diurnal chemical fluctuations on the scattering properties can be addressed as well.

The merging of the SMPS and APS measurements is something that definitely needs more attention. The merging was done by eye, but more accurate merging procedures do exist. Algorithms which find the best fit between two instrument data sets are used in literature (e.g., (Beddows et al., 2010)). Also, the translation from aerodynamic diameter to volume equivalent particle diameter can be different for every moment in time as it depends on the aerosol density. But, this study used a fixed value for the aerosol density for all measurements within the same campaign. It would be beneficial if this value is optimized for every measuring moment. Furthermore and even more important, the last model runs with TROLIX data used APS and SMPS data that did not merge well. An aerosol effective density of 2.4 g/cm³ had to be assumed to create a continuous PSD. This density is really high compared to the expected APS aerosol density and seems to indicate that one or both of the instruments might have a (small) error whilst measuring. Add to this the fact that the SMPS also had problems measuring small particles, a calibration of the SMPS would clarify whether or not the PSD may be unrealistic. A slightly changed or shifted SMPS PSD could create a better merging with the APS and result in a merged PSD with more and larger particles. With the test runs it was shown that a change in the numbers of aerosols with a large diameter do affect the scattering significantly. Especially larger particles in the PSD could reduce the difference between the calculations and the measurements.

From the results in Figure 4.30c, it can be seen that aerosols particles with a radius between 0.1 and 1 μm contribute significantly to the scattering coefficient. This range can become larger if the PSD contains more larger particles as it depends on the total particle number and its cross section. However, the peak is expected to be always near this range in standard dutch aerosol conditions (when RH<100%). This radius range is however centered around the location which is defined by the merging of the APS and SMPS of which we are not certain. It is therefore recom-

mended for future researches to use an SMPS that can measure a PSD up to approximately 800 nm or more, so that uncertainties due to merging can be reduced. Most importantly is, that if the SMPS and APS measurements have to be combined, that the measurements of APS and MSP overlap in range so that merging both data sets becomes much more reliable.

5.1.3 Discussion on the nephelometers

The nephelometer results are used as the ground truth during the validation of the H-model. However, it is possible that the nephelometer results do not represent the true value as it is, which would make the validation between the H-model and nephelometers a lot more complicated. In this discussion we will mainly focus on the nephelometers used during the TROLIX campaign, as the main results of this study are based on the validation of the H-model with TROLIX data. During this study, three possible nephelometer uncertainties might have influenced the results:

During the nephelometer data processing, a bias was found between the two different instruments. A difference of almost 20% was observed between the scattering coefficients of both instruments, which should have been 5% maximum. Therefore it was decided to scale the results of one of the nephelometers so that the bias was removed: The scattering coefficients of the old nephelometer were divided by 1.21. However, this decision to scale the values of the old nephelometer was simply based on the age of the nephelometer expecting that the new nephelometer would be more accurate, for which is no direct proof. By simply scaling these scattering coefficients without any extra calibration, the comparison between the measured scattering coefficients and calculated scattering coefficients shown in Figure 4.17 (bottom figure) becomes more meaningless in scale (not in correlation). The scaling itself has the advantage that the enhancement factors of the nephelometers become more reliable, so the comparison between the calculated and measured enhancement factors is more important than the comparison between the scattering coefficients. The most important conclusion would be that a difference of almost 20% between the two nephelometers is really high. For a followup study it would be recommended to use one nephelometer which both measures dry and enhanced values so that at least the enhancement factor is reliable. For this study it would be good to calibrate both nephelometers again and use the outcome to correct the results.

Another possibility to explain the difference in scattering and enhancement factors between the H-model and the WetNeph measurements, is that the internal sensors of the nephelometer do not measure the exact RH or temperature at the sensing volume itself. As a final model run it can be concluded that if the air would be 4 degrees warmer inside the sensing volume of the WetNeph and it would have enough time to reach a new RH equilibrium, the mean enhancement values of the WetNeph and H-model would overlap. It might be possible that the temperature sensor and RH sensor do not measure the exact values of the internal conditions or that these are slightly biased.

Also, the temperature and RH sensors of the nephelometers show some strange values if the sensors of both nephelometers are compared to each other. Especially the temperature sensors show some unlikely behaviour during the parallel measurements, as the measured temperatures between both nephelometers differ significantly from each other, also at the input measurements. It is not known when both sensors were last calibrated. A calibration of the RH and temperature sensors is needed to interpret the results better.

5.2 Conclusions

The H-model seems to be able to calculate atmospheric scattering properties based on dry in situ aerosol measurements including chemical composition, particle size distribution, temperature and relative humidity. Changes in chemical composition or PSD influence the scattering properties in a similar way as measured by the WetNeph measurements, as they have a strong correlation. Ignoring the difference in magnitude, the scattering enhancement estimated by the H-model follows the same trends as the scattering enhancement measured by the WetNeph. The dependencies on chemical composition, PSD and RH are similar. However, the resulting values of the scattering coefficients and enhancement factors still don't match as the magnitude of both results are not the same. As described in the discussion there are some adjustments and recommendations to improve the validation process. Most of these suggested improvements are aimed at making the calculated result more precise instead of accurate. They will not solve the problem of difference between the calculations and the measurements of the scattering properties.

With the current data it is not possible to make a fair judgement on the true accuracy of the results. This concerns both the calculated values by the model, but also the measured values by the WetNeph. The particle size distribution which is used as input for the H-model, might be inaccurate as doubtful assumptions had to be made to merge the SMPS and APS distribution. The region where the APS and SMPS are merged, turns out to be the most significant region of particle sizes for the scattering coefficient (and thus enhancement factor). The test results showed that a PSD with relatively more larger particles resulted in enhancement factors closer to those of the WetNeph. If the PSD is erroneously taken as correct, this could influence the results and thus the conclusions. Something similar also applies to the WetNeph. The results from the WetNeph are used as the true values. However, deviations within the internal temperature or RH could explain the differences in the validation results and a large adjustment between both nephelometers has to be made in order to calculate realistic enhancement factors. Also temperature and RH differences between both nephelometers raise some questions. For both the SMPS and WetNeph, it would be strongly recommended to recalibrate the instruments. By doing so, a better judgement can be made about the accuracy of the results.

Based on current data comparisons, the H-model does not yet meet the expected results. There is not yet sufficient closure between measured and calculated scattering properties. However, it can be concluded that the results from the H-model are promising. The translation from dry in situ measurements to enhanced values is well captured by ISORROPIA and a clear correlation between the calculated and measured enhancement factor is observed.

A List of acronyms and abbreviations

APS	Aerodynamic Particle Sizer
BC	Black Carbon
CINDI	Cabauw Intercomparison of Nitrogen Dioxide measuring Instruments
EC	Elemental Carbon
$f(RH, \lambda)$	Scattering enhancement factor
GC-MS	Gas Chromatography Mass Spectrometry
MAAP	Multi-Angle Absorption Photometer
MARGA	Monitor for AeRosols and Gases in ambient Air
OC	Organic Carbon
PSD	Particle Size Distribution
RH	Relative humidity
RI	Refractive Index
RIVM	RijksInstituut voor Volksgezondheid en Milieu
SIA	Secondary Inorganic Aerosol
SMPS	Scanning Mobility Particle Sizer
SOA	Secondary Organic Aerosol
SS	Sea Salt
TROLIX	TROpomi vaLIdation eXperiment
UTC	Coordinated Universal Time
WetNeph	Humidified Nephelometer

D_a	Aerodynamic diameter of an aerosol particle
D_p	Diameter of an aerosol particle
g_D	Diameter growth factor
$g(RH)$	Hygroscopic growth factor
g_v	Volume growth factor
G	Aerosol cross section
N	Number of aerosol particles
Q_{ext}, Q_e	Extinction efficiency
Q_{sca}, Q_s	Scattering efficiency
V	Volume

λ	Wavelength
ρ_{eff}	Effective density
σ_a	Absorption coefficient
σ_e	Extinction coefficient
σ_s	Scattering coefficient

List of Figures

2.1	Example of the efficiency $Q(\sigma/\pi r^2)$ as a function of the size parameter $(\frac{2\pi r}{\lambda})$ for RI=1.5 0.02i.	4
2.2	Example of efficiency $Q(\sigma/\pi r^2)$ as a function of the aerosol particle radius [μm] for RI=1.5 0.02i.	4
2.3	Example of the deliquescent behaviour of a NaCl particle: 2D area growth of NaCl as a function of RH. (Gupta et al., 2015)	5
2.4	Example of an aerosol mixture whose growth factor is influenced by the presence of aerosols with a deliquescent behaviour: Diameter growth factor (G) as a function of RH. (Boreddy et al., 2014)	5
3.1	Components and steps of the H-model for calculating scattering properties based on in situ measurements.	7
3.2	PSD divided into 100 log-scale bins.	9
3.3	Example of the PSD based on SMPS and APS measurements after merging both data sets, divided into 100 log-scale bins.	12
3.4	Example PSD for different values of RH based on total-volume growth. The PSD of RH=0 and RH=25 are overlapping.	13
4.1	Example of a combined PSD from the SMPS and APS (left: original, right: adjusted).	15
4.2	Enhancement factor $f(\text{RH}=85)$ ($\lambda = 550\text{nm}$) measured by the WetNeph and calculated by the H-model during the campaign.	17
4.3	Collection of all $f(\text{RH})$ calculations by the H-model ($\lambda = 550\text{nm}$).	17
4.4	Mass concentration of different aerosol species at all measuring moments compared to the final enhancement factor $f(\text{RH}=85)(\lambda = 550\text{nm})$	18
4.5	Mass concentration of different aerosol species at all measuring moments.	18
4.6	Volume and diameter growth factor as a function of RH as predicted by ISORROPIA.	20
4.7	Enhancement factor ($\lambda = 550\text{nm}$) as a function of RH according to ISORROPIA sensitivit results in combination with the H-model.	20
4.8	Variations of a chemical aerosol mixture with the same PSD (and same total volume). Top bar graph shows the dry chemical mixture. Bottom bar graph shows the chemical mixture at 85% relative humidity including water calculated by the model.	21
4.9	The enhancement factor ($\lambda = 550\text{nm}$) calculated by the model based on variations of a standard chemical mixture of aerosols with the same PSD.	22
4.10	Mean PSD during the campaign based on the chosen ρ_{eff}	23
4.11	RH measured by both setups. Until 11 September, both setups measured the same air. After 11 September the air is dried or enhanced for the dry- and wet-setup respectively.	25
4.12	σ_s as measured by both nephelometer instruments during the test period only.	25
4.13	Comparison between the scattering coefficients of both nephelometer instruments (old and new) during parallel measuring in dry conditions (7-10 September 2019 for $\lambda = 550\text{nm}$). The trend which can be found is ignored as it is too small to have a significant effect.	26
4.14	Hourly mean scattering coefficient measured in dry conditions and with enhanced RH ($\lambda = 550\text{nm}$) [Top]. Including the scattering enhancement factor for each specific measurement moment [Bottom].	26
4.15	Mass and volume comparison of different measurement techniques during the entire campaign period	29
4.16	Diameter growth factor (using ISORROPIA and κ -Köhler theory), including the enhanced RH on which the growth factors are based.	29
4.17	Enhancement factors and scattering coefficients as measured by the WetNeph and calculated by the H-model (using ISORROPIA and κ -Köhler theory for $\lambda = 550\text{nm}$).	30
4.18	Comparison of the $f(\text{RH})$ results. (The H-model includes ISORROPIA.)	31
4.19	Comparison of the $f(\text{RH})$ results. (The H-model includes the Kappa approach.)	31
4.20	The difference between $f(\text{RH})$ calculated and $f(\text{RH})$ measured as a function of RH. (The H-model includes ISORROPIA.)	31

4.21	The difference between $f(\text{RH})$ calculated and $f(\text{RH})$ measured as a function of RH. (The H-model includes the Kappa approach.)	31
4.22	The enhancement factor split up into cross section enhancement and scattering efficiency enhancement (using $\lambda = 550\text{nm}$).	32
4.23	Example of the aerosol scattering efficiency of a single aerosol particle (dry or wet) as a function of its radius (for $\lambda = 550\text{nm}$). The graph is a smoothed visualization.	33
4.24	Measured scattering enhancement(WetNeph) versus calculated scattering enhancements (κ -Köhler) based on the RH measured by the WN and 0.8 times the RH ($\lambda = 550\text{nm}$).	33
4.25	Comparison between measured (by the WetNeph) and calculated (by the H-model) enhancement factors. The H-model uses the original RH values (as measured by the WetNeph) and decreased RH ($0.80 \cdot \text{RH}$). (The H-model includes the Kappa approach.)	34
4.26	The difference between $f(\text{RH})$ calculated and $f(\text{RH})$ measured as a function of RH. The model uses the original RH values (as measured by the WetNeph) and decreased RH ($0.80 \cdot \text{RH}$). (The H-model includes the Kappa approach.)	34
4.27	Aerosol scattering enhancement ($\lambda = 550\text{nm}$). The figure shows $f(\text{RH})$ as measured by the WetNeph (black line) and the original calculation by the H-model (red line). In addition the H-model calculated the $f(\text{RH})$ for a PSD with no small aerosol particles (dashed cyan line) and the $f(\text{RH})$ for a PSD which includes more larger particles (solid cyan line).	35
4.28	Comparison between measured (by the WetNeph) and calculated (by the H-model) enhancement factors. The H-model uses the original PSD (APS $\rho_{eff}=2.4$) and PSD with an increased amount of large particles (APS $\rho_{eff}=2.0$). (The H-model includes the Kappa approach)	35
4.29	The difference between $f(\text{RH})$ calculated and $f(\text{RH})$ measured as a function of RH. The H-model uses the original PSD (APS $\rho_{eff}=2.4$) and PSD with an increased amount of large particles (APS $\rho_{eff}=2.0$). (The H-model includes the Kappa approach)	35
4.30	Example of the bin-wise calculation of the scattering coefficient based on the scattering efficiency (Q_{scat} and cross section G). Sub-figure A shows the original and wet PSD in dry and wet conditions in combination with the dry and wet scattering efficiency curve. Sub-figure B shows the total cross section per bin for all PSDs in combination with the dry and wet scattering efficiency curve. Sub-Figure C shows the scattering coefficient per bin for all PSDs.	38

List of Tables

3.1	Basic information on measured aerosols species needed as input for the H-model.	10
3.2	Composition of sea salt; based on seawater composition and ignoring atmospheric transformation (Seinfeld and Pandis, 2006).	11
3.3	Refractive index of different aerosol composition ($\lambda \approx 550\text{nm}$) ((Kim et al., 2015), (Seinfeld and Pandis, 2006), (Shettle and Fenn, 1979), (Hess et al., 1998))	12
4.1	Basic information on estimated aerosols species as measured or assumed during the CINDI campaign 2009.	16
4.2	During the TROLIX campaign, aerosol measurements were taken at Cabauw for 4 weeks. Days coloured in red have an incomplete data set, days coloured in dark green have a complete data set and are used in this study, days in light green have a complete data set which is not yet available.	22
4.3	Basic information on estimated aerosols species as measured or assumed during the CINDI campaign 2009	24
4.4	Hygroscopic coefficient κ per aerosol species (Petters and Kreidenweis, 2007)	27
4.5	Scattering properties of the 'original' PSD (as shown in Figure 4.30)	36
4.6	Scattering properties of the 'large' PSD (as shown in Figure 4.30)	36

Bibliography

- Alduchov, O. A. and Eskridge, R. E. (1996). Improved magnus form approximation of saturation vapor pressure. *Journal of Applied Meteorology*, 35(4):601–609.
- Beddows, D. C., Dall'osto, M., and Harrison, R. M. (2010). An enhanced procedure for the merging of atmospheric particle size distribution data measured using electrical mobility and time-of-flight analysers. *Aerosol Science and Technology*, 44(11):930–938.
- Bergström, R., Denier Van Der Gon, H., Prévôt, A. S., Yttri, K. E., and Simpson, D. (2012). Modelling of organic aerosols over europe (2002–2007) using a volatility basis set (vbs) framework: application of different assumptions regarding the formation of secondary organic aerosol. *Atmospheric Chemistry and Physics*, 12(18):8499–8527.
- Boreddy, S., Kawamura, K., and Jung, J. (2014). Hygroscopic properties of particles nebulized from water extracts of aerosols collected at chichijima island in the western north pacific: An outflow region of asian dust. *Journal of Geophysical Research: Atmospheres*, 119(1):167–178.
- Buijsman, E., Cassee, F., Fischer, P., Hoogerbrugge, R., Maas, R., van der Swaluw, E., and van Zanten, M. (2013). Dossier fijn stof. *Bilthoven, Rijksinstituut voor Volksgezondheid en Milieu (RIVM)*.
- Fountoukis, C. and Nenes, A. (2007). ISORROPIA II: a computationally efficient thermodynamic equilibrium model for $K^+ - Ca^{2+} - Mg^{2+} - NH_4^+ - Na^+ - SO_4^{2-} - NO_3^- - Cl^- - H_2O$ aerosols. *Atmospheric Chemistry and Physics*, 7(17):4639–4659.
- Guo, L., Gu, W., Peng, C., Wang, W., Li, Y. J., Zong, T., Tang, Y., Wu, Z., Lin, Q., Ge, M., et al. (2019). A comprehensive study of hygroscopic properties of calcium-and magnesium-containing salts: implication for hygroscopicity of mineral dust and sea salt aerosols. *Atmospheric Chemistry and Physics*, 19(4):2115–2133.
- Gupta, D., Eom, H.-J., Cho, H.-R., and Ro, C.-U. (2015). Hygroscopic behavior of NaCl- $MgCl_2$ mixture particles as nascent sea-spray aerosol surrogates and observation of efflorescence during humidification. *Atmospheric Chemistry and Physics*, 15(19):11273–11290.
- Hess, M., Koepke, P., and Schult, I. (1998). Optical properties of aerosols and clouds: The software package OPAC. *Bulletin of the American meteorological society*, 79(5):831–844.
- Kazadzis, S. (2016). WMO/GAW aerosol measurement procedures, guidelines and recommendations. Technical report, Tech. rep., World Meteorological Organization.
- Kim, J., Bauer, H., Dobovičnik, T., Hitzenberger, R., Lottin, D., Ferry, D., and Petzold, A. (2015). Assessing optical properties and refractive index of combustion aerosol particles through combined experimental and modeling studies. *Aerosol Science and Technology*, 49(5):340–350.
- Latimer, R. and Martin, R. (2019). Interpretation of measured aerosol mass scattering efficiency over north america using a chemical transport model. *Atmospheric Chemistry and Physics*, 19:2635–2653.
- Manders, A., Schaap, M., Jozwicka, M., Van Arkel, E., Weijers, E., and Matthijsen, J. (2009). The contribution of sea salt to PM10 and PM2.5 in the netherlands. *BOP report*, 500099004.
- Myhre, G., Shindell, D., Breon, F.-M., Collins, W., Fuglestedt, J., Huang, J., Koch, D., Lamarque, J.-F., Lee, D., Mendoza, B., Nakajima, T., Robock, A., Stephens, G., Takemura, T., and Zhang, H. (2013). *Anthropogenic and Natural Radiative Forcing*, book section 8, page 659–740. Cambridge University Press, Cambridge, United Kingdom and New York, NY, USA.
- Petters, M. and Kreidenweis, S. (2007). A single parameter representation of hygroscopic growth and cloud condensation nucleus activity. *Atmospheric Chemistry and Physics*, 7(8):1961–1971.

- Pinterich, T., Spielman, S., Wang, Y., Hering, S., and Wang, J. (2017). A humidity-controlled fast integrated mobility spectrometer (HFIMS) for rapid measurements of particle hygroscopic growth. *Atmospheric Measurement Techniques*, 10:4915–4925.
- Rooij de, W. A. and Stap van der, C. (1987). Expansion of mie scattering matrices in generalized spherical functions. *Astronomy and Astrophysics*, 131:237–248.
- Seinfeld, J. H. and Pandis, S. N. (2006). *Atmospheric chemistry and physics: From air pollution to climate change*. John Wiley & Sons.
- Shettle, E. P. and Fenn, R. W. (1979). Models for the aerosols of the lower atmosphere and the effects of humidity variations on their optical properties. Technical report, Air Force Geophysics Lab, Hanscom Air Force Base, Mass.
- Topping, D., Coe, H., McFiggans, G., Burgess, R., Allan, J., Alfarra, M., Bower, K., Choularton, T., Decesari, S., and Facchini, M. C. (2004). Aerosol chemical characteristics from sampling conducted on the island of jeju, korea during ace asia. *Atmospheric Environment*, 38(14):2111–2123.
- Wang, Z., Cheng, Y., Ma, N., Mikhailov, E., Pöschl, U., and Su, H. (2017). Dependence of the hygroscopicity parameter κ on particle size, humidity and solute concentration: implications for laboratory experiments, field measurements and model studies. *Atmospheric Chemistry and Physics Discussions*, 2017:1–33.
- Wise, M. E., Surratt, J. D., Curtis, D. B., Shilling, J. E., and Tolbert, M. A. (2003). Hygroscopic growth of ammonium sulfate/dicarboxylic acids. *Journal of Geophysical Research: Atmospheres*, 108(D20).
- Zieger, P., Fierz-Schmidhauser, R., Weingartner, E., and Baltensperger, U. (2013). Effects of relative humidity on aerosol light scattering: results from different european sites. *Atmospheric Chemistry and Physics*, 13(21):10609–10631.
- Zieger, P., Weingartner, E., Henzing, J., Moerman, M., Leeuw, G. d., Mikkilä, J., Ehn, M., Petäjä, T., Clémer, K., Roozendaal, M. v., et al. (2011). Comparison of ambient aerosol extinction coefficients obtained from in-situ, MAX-DOAS and LIDAR measurements at cabauw. *Atmospheric Chemistry and Physics*, 11(6):2603–2624.